

**THEORETICAL AND EXPERIMENTAL ASSESSMENT  
OF THE VIABILITY OF 1,4,6,9-SPIRO[4.4]NONATETRAYL  
AS A REACTIVE INTERMEDIATE**

Thesis by  
**Lisa Ann McElwee-White**

In Partial Fulfillment of the Requirements  
for the Degree of  
Doctor of Philosophy

California Institute of Technology  
Pasadena, California

**1984**

(Submitted October 17, 1983)

TO MY PARENTS

AND

TO JIM

## ACKNOWLEDGEMENTS

My warmest thanks go to Dennis Dougherty, who has been as much a friend as an advisor. Help was always there whenever I needed it, but I was allowed to learn and grow in my own way. I shall miss our long conversations, but I can leave knowing I learned to do things the right way.

The Dougherty group will always be special to me. The scientific exchange was marvelous, as were the friendships. I am grateful to Aaron "they call me Gomez" Goldberg and Gary "Mr. Microwaved HH" Snyder for assistance with the ESR spectra. Also, thanks to first Mike Petti and then Tim Shepodd for buying a certain 9 foot yellow couch.

Bill Goddard and his group were invaluable to the theoretical portion of this thesis. John Low, Art Voter and Marv Goodgame were never too busy to talk theory to an often confused organic experimentalist. They saved me from endless hours of frustration.

I am also grateful for the advice, equipment loans, scientific exchange and social life provided by Peter Dervan and his group. Ditto for the Bercaw group with special thanks to Chris, Tippy and DMR who smiled bravely when I used their Toepler pumps. All of the other people who made my stay at Caltech worthwhile are too numerous to mention, but you know who you are, especially Maile, who always wanted to be in someone's thesis.

Financial support for my graduate work was provided first by Caltech, in the form of an Institute Fellowship and then by the National Science Foundation as a Predoctoral Fellowship.

Thanks also to Gwen Anastasi, who typed this manuscript so very well.

And to the Sweetie: "Isle of Ewe".

ABSTRACT

Qualitative molecular orbital (MO) theory predicts that 1,4,6,9-spiro[4.4]nonatetrayl (7) should be stabilized via spiroconjugative interaction of the four radical p orbitals. In addition to this thermodynamic stabilization, energetic barriers are predicted for closure to either of the closed shell forms.

The electronic structure of 7 has been investigated using ab initio electronic structure theory. The spiroconjugative interaction of the four radical centers is evidenced by a large orbital splitting. However, spiroconjugation does not confer upon the structure the electronic properties of a biradical, contrary to qualitative MO considerations. Structure 7 possesses the six, low-lying (covalent) states that characterize a tetraradical. Spiroconjugation does strongly influence the relative energies of these six states, and does lead to a small but significant stabilization of the molecule. Possible modes of ring closure and closed shell isomers of 7 are also discussed.

Direct photolysis of spiro[bis(2,3-diazabicyclo[2.2.1]hept-2-ene)-7,7'] (17) leads to loss of a single equivalent of N<sub>2</sub> and ring closure of the resulting biradical to 2,3-diazabicyclo[2.2.1]hept-2-ene-7,5'-spirobicyclo[2.1.0]pentane (19). Generation of the triplet biradical by sensitized photolysis results in a competition between ring

closure to 19 and a 1,2-alkyl shift to 8,9-diazatricyclo-[5.2.2.0<sup>2,6</sup>]undeca-2,8-diene (23). While direct photolysis and thermolysis of 19 yield primarily ring closure product, sensitized photolysis leads to a series of biradical-to-biradical rearrangements that ultimately produce 2,3-divinylcyclopentene (24). Deuterium labeling studies indicate competing mechanistic pathways for this reaction. Rationalization of the label distribution requires one of two unprecedented processes: frontside radical attack on a C-C bond or intermediacy of 1,4,6,9-spiro[4.4]nonatetrayl.

## TABLE OF CONTENTS

	<u>Page</u>
List of Figures . . . . .	ix
List of Tables . . . . .	x
Chapter I.     RATIONAL DESIGN OF AN ORGANIC TETRARADICAL. .	1
References for Chapter I. . . . .	10
Chapter II.    THEORETICAL STUDIES ON 1,4,6,9-SPIRO[4.4]- NONATETRAYL . . . . .	12
A.   MNDO Study of the Ring Opening of Bicyclo[2.1.0]pentanes . . . . .	13
B.   Qualitative Molecular Orbital Analysis of Spirononatetrayl. The Biradical Model . . . .	17
C.   Qualitative Valence Bond Analysis of Spirononatetrayl. The Tetraradical Model . . .	19
D. <u>Ab Initio</u> Computational Methods . . . . .	22
E.   Results and Discussion for <u>Ab Initio</u> Studies on Spirononatetrayl . . . . .	24
F.   Conclusions . . . . .	42
References for Chapter II . . . . .	46
Chapter III.   EXPERIMENTAL ASSESSMENT OF THE VIABILITY OF 1,4,6,9-SPIRO[4.4]NONATETRAYL AS A REACTIVE INTERMEDIATE . . . . .	48
A.   Potential Precursors to Spirononatetrayl . . .	49
B.   Synthesis of Precursor Diazenes . . . . .	51
C.   Results and Discussion for Diazene Decompositions. Biradical to Biradical Rearrangements . . . . .	53
D.   Electron Spin Resonance Studies of Diazene Decompositions . . . . .	74

	<u>Page</u>
E. Conclusions . . . . .	89
F. Experimental Section . . . . .	91
References and Notes for Chapter III . . . . .	106



## LIST OF FIGURES

	<u>Page</u>
Figure 1. Orbital Mixing Diagram for 1,4,6,9-Spiro[4.4]nonatetrayl . . . . .	5
Figure 2. Orbital Mixing Diagram for 1,3,6,8-Spiro[4.4]nonatetraene . . . . .	6
Figure 3. Partially Localized Orbitals of <u>13a</u> . . . . .	31
Figure 4. Relative Energies of the States of <u>13a</u> from RCI and CI-VDZ Calculations . . . . .	35
Figure 5. Relative Energies of the States of <u>13a</u> and Forms Distorted by the Second Order Jahn-Teller Effect . . . . .	44
Figure 6. Relative Molar Ratios of Products from the Sensitized Photolysis of <u>17</u> . . . . .	54
Figure 7. $^2\text{H}$ NMR of <u>24</u> Derived from the Sensitized Photolysis of <u>19b</u> . . . . .	63
Figure 8. $^2\text{H}$ NMR of <u>24</u> Derived from the Sensitized Photolysis of <u>19c</u> . . . . .	66
Figure 9. ESR Spectrum Obtained upon Irradiation of a MTHF Matrix Containing <u>19</u> at 8 K . . . . .	75
Figure 10. Curie Plot for the Triplet Species Generated upon Photolysis of <u>19</u> . . . . .	77
Figure 11. ESR Spectrum Obtained upon Irradiation of a MTHF Matrix Containing <u>23</u> at 8 K . . . . .	84

## LIST OF TABLES

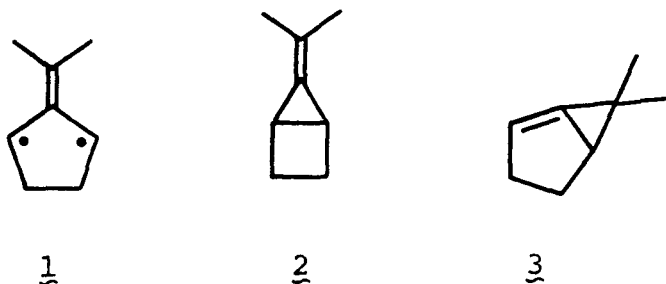
	<u>Page</u>
Table I. MNDO Heats of Formation for Points along the Conversion of <u>6</u> to <u>4</u> . . . . .	15
Table II. MNDO Heats of Formation for Points along the Conversion of <u>11</u> to <u>7</u> . . . . .	16
Table III. Relative Energies (kcal/mol) for Covalent States of <u>13</u> . . . . .	26
Table IV. CI-VDZ Wavefunctions for Covalent States of <u>13</u> . . . . .	27
Table V. Relative Energies (eV) for States of <u>13</u> . . . . .	28
Table VI. CI-VDZ Wavefunctions of <u>13a</u> Using the Partially Localized Orbitals of Figure 3 . . . . .	32
Table VII. Relative Energies (kcal/mol) of the Covalent States of <u>15</u> and <u>16</u> . . . . .	43
Table VIII. Quantum Yields for Sensitized Photolysis of Diazenes . . . . .	57
Table IX. Product Yields from <u>19</u> and <u>23</u> . . . . .	58
Table X. Distribution of <sup>2</sup> H in <u>24</u> . . . . .	64
Table XI. Relative Rates for Biradical-to- Biradical Rearrangements Leading to <u>24</u> . . . . .	73
Table XII. Zero Field Splitting Parameters for Biradicals Derived from Various Diazenes . . . . .	78
Table XIII. Zero Field Splitting Parameters for Various Biradicals . . . . .	80

CHAPTER I.

Rational Design of an Organic Tetraradical

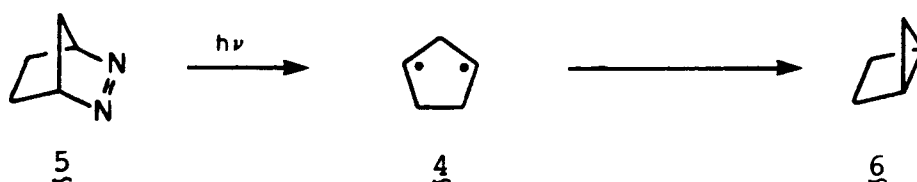
Because chemical reactions involve the breaking and making of bonds, organic chemists have sought to observe and characterize species containing carbon atoms of unusual valence in hopes of gaining insight into reaction mechanisms. One type of hypovalent species is the biradical, a molecule with one fewer bond than the standard rules of valence allow.<sup>1</sup> Interest in the pathways of both thermal<sup>2</sup> and photochemical<sup>3</sup> rearrangements has led to substantial activity in the field of biradicals as evidenced by a recent symposium-in-print<sup>4</sup> and monograph<sup>5</sup> on the subject.

Biradicals are by nature highly reactive, making their observation and characterization a challenging problem. Bond-broken species designed for direct observation have usually possessed one or both of the following characteristics: destabilization of their open shell isomers by the introduction of high strain energy and stabilization of the non-bonding electrons by conjugation with a  $\pi$  system. Among the most elegant examples of this strategy are Berson's studies on trimethylenemethane derivative 1.<sup>1,6</sup> Inclusion of the biradical moiety in a five-membered ring destabilizes the closed shell isomers 2 and 3 to the extent that both singlet and triplet 1 live long enough at



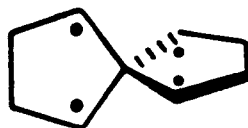
-78°C to undergo intermolecular trapping by olefins. In addition, both spin states have been observed spectroscopically, the triplet by ESR<sup>6</sup> and the singlet by picosecond fluorescence spectroscopy.<sup>7</sup>

High strain of the closure products has also been used to advantage by Closs in his study of 1,3-cyclopentadienyl (4).<sup>8</sup> Irradiation of 2,3-diazabicyclo[2.2.1]hept-2-ene (5) in a matrix at 5.5 K led to the ESR signal of triplet biradical 4. Although tunneling contributed to decay of the



signal at low temperatures, conventional ring closure of 4 to the highly strained bicyclo[2.1.0]pentane (6) required surmounting a 2.3 kcal/mol barrier, rendering 4 the first observable localized 1,3-biradical.

The successful observation of 4 led to consideration of 1,4,6,9-spiro[4.4]nonatetrayl (7) as a candidate for direct



observation and characterization. As shown in Figure 1, 7 can be viewed as a pair of cyclopentanedyl fragments, linked by a common carbon which forces the two rings to be perpendicular. The special topology of the spiro ring system leads to interaction of the cyclopentanedyl fragment orbitals in 7. By symmetry the  $b_1$  orbitals of 4 cannot mix, and they give rise to a degenerate pair of non bonding molecular orbitals (NBMO) designated e in the  $D_{2d}$  symmetry of 7. However, the  $a_2$  orbitals of 4 do mix, leading to a stabilized  $b_1$  orbital and a destabilized  $a_2$  orbital.

This type of interaction between perpendicular sets of p orbitals in spiro ring systems has been dubbed spiroconjugation.<sup>9</sup> Experimental evidence for this phenomenon can be found in the photoelectron spectrum of 1,3,6,8-spiro-[4.4]nonatetraene<sup>10</sup> (8) for which an orbital mixing diagram is shown in Figure 2. The first two ionization bands of 8 are split by 1.23 eV, indicating the difference in energy between the  $a_2$  and  $b_1$  orbitals. Additional evidence for spiroconjugative interaction occurs in the heat of hydrogenation for 1,1'-spirobiindene.<sup>11</sup> Reduction of the spiro compound releases 13.7 kcal/mol more energy than hydrogenation of two indenenes, indicating spiroconjugative destabilization by that amount.

Photoelectron spectroscopic studies of spirononatetraene derivatives led Schweig to propose the empirical formula shown in eq. 1 for the prediction of spiroconjugative splitting in such compounds.<sup>12</sup> The orbital split  $\Delta E$  is calculated in

FIGURE 1. Orbital Mixing Diagram for 1,4,6,9-Spiro-[4.4]nonatetrayl

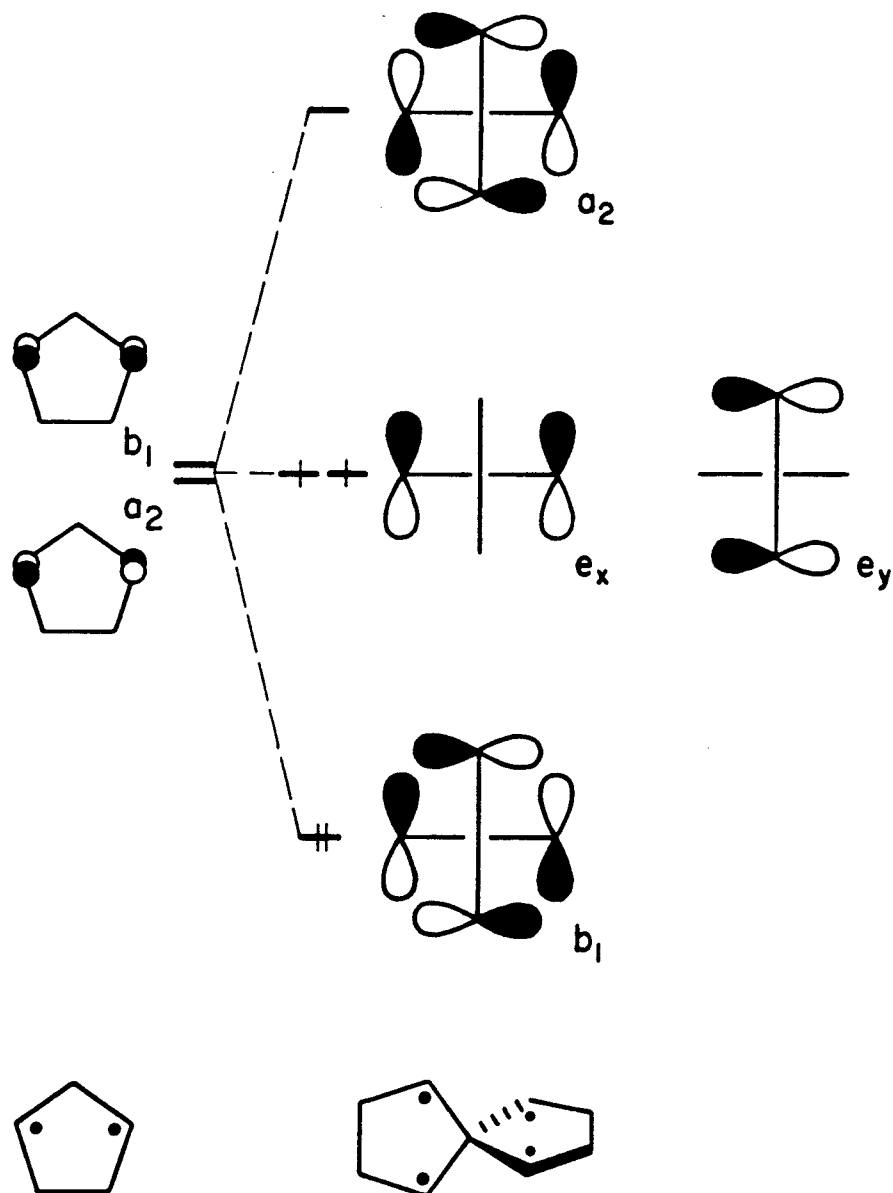
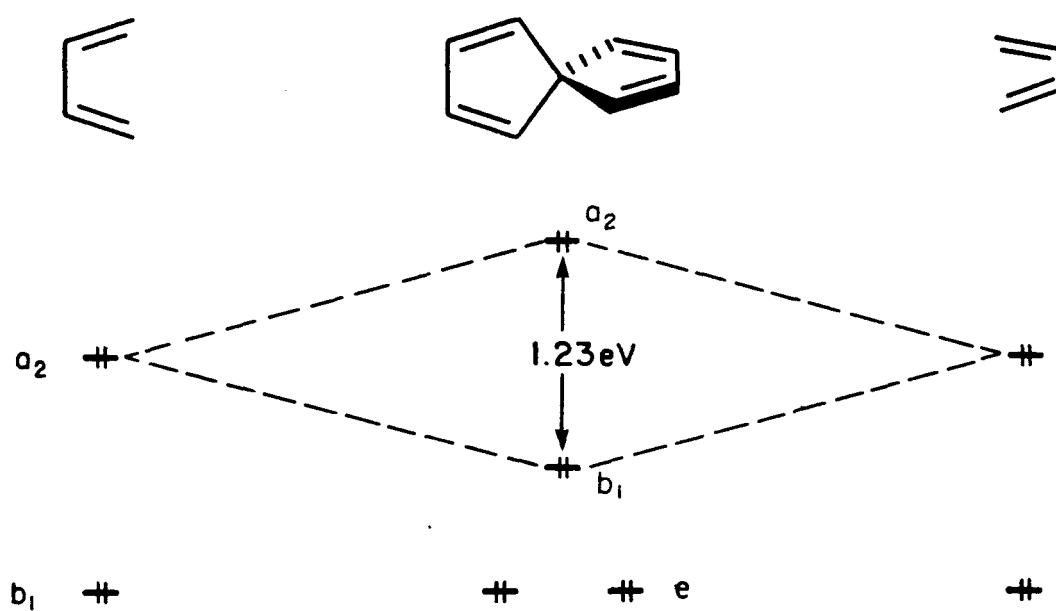


FIGURE 2. Orbital Mixing Diagram for 1,3,6,8-Spiro[4.4]nonatetraene





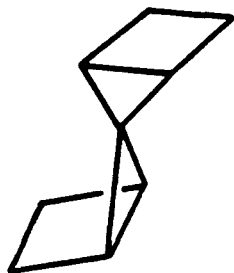
$$\Delta E = 2(C_1C_2 - C_1C_4 - C_2C_3 + C_3C_4)\beta \quad (1)$$

terms of  $\beta$ , an empirically determined constant and the coefficients ( $C_1$ - $C_4$ ) of the p orbitals in the unperturbed fragments as calculated by an NDO method. Applying this formula to spirononatetrayl 7 leads to a prediction of a 1.96 eV split between the  $b_1$  and  $a_2$  orbitals, if coefficients  $C_1$ - $C_4$  are assumed to be  $1/\sqrt{2}$ . Although the coefficients of the cyclopentanedyl fragment p orbitals will be slightly smaller than  $1/\sqrt{2}$  due to electron density on the methylene through bond coupling unit,<sup>13</sup> Schweig's formula predicts substantial spiroconjugative interaction for 7.

Thus, symmetry considerations dictate a mixing of the radical p orbitals of 7 and eq. 1 predicts the resulting  $b_1$ - $a_2$  gap to be significant. MO theory then suggests the orbital occupation shown in Figure 1, with the stabilized  $b_1$  orbital doubly occupied and two electrons in the e orbitals. At the level of one electron theory, 7 is predicted to be stabilized relative to a molecule with four electrons in four NBMO's by  $2(1.96 \text{ eV}/2) = 1.96 \text{ eV}$  or 45 kcal/mol. Note also that this electronic structure for 7 also fits one definition of a biradical - a molecule with two electrons in a pair of degenerate NBMO.<sup>14</sup>

In addition to stabilization of non-bonding electrons, the design of 7 incorporates high strain energy in the closed shell isomers. There are two possible modes of ring closure

for 7. A double disrotatory closure of the individual 1,3-cyclopentanedyl fragments leads to spiro[bis(bicyclo-[2.1.0]pentane)-5,5'] (9). The alternative radical coupling would produce tetracyclo[4.3.0.0.<sup>1,5</sup><sub>0</sub><sup>2,9</sup>]nonane ([5.3.5.3]-fenestrane, 10). Using bicyclo[2.1.0]pentane as a model for

910

9, the strain energy can be estimated as  $2 \times 57 \text{ kcal/mol}$  (twice the strain of 6)<sup>15a</sup> +  $10 \text{ kcal/mol}$  (difference in strain between spiropentane and two cyclopropanes<sup>15b</sup>) =  $124 \text{ kcal/mol}$ . Geometry optimization of 10 using MNDO<sup>16</sup> and calculations on the optimized structure gave a heat of formation of  $110.5 \text{ kcal/mol}$ , leading to a strain energy of  $139 \text{ kcal/mol}$ . Despite uncertainty in the accuracy of this semi-empirical method when applied to such a distorted molecule, it seems clear that the strain energy of 10 would be quite high. Since 7 would be very nearly strain-free and stabilized by spiroconjugation, a ring closure to either 9 or 10 should possess a relatively small thermodynamic driving force, compared to what one would expect for the conversion of a "typical" tetraradical to a closed-shell molecule. One can also anticipate possible kinetic barriers to such ring closures. An orbital correlation diagram for double ring closure of 7 to 9 shows that the e orbitals of 7 correlate

with the developing  $\sigma$  bonds of 9, while the stabilized  $b_1$  orbital correlates with a  $\sigma^*$  orbital. Such a closure is thus forbidden in the sense of the "natural orbital correlations",<sup>17</sup> and a barrier to the process would be expected. The early stages of the conversion of 7 to 10 correspond to a second order Jahn-Teller distortion mode. Ab initio calculations (see Chapter II) suggest that such a motion is energetically unfavorable, and thus this process, too, should have an activation energy.

To summarize, tetraradical 7 would be stabilized to some extent by spiroconjugation. Both closed shell isomers of 7 would be highly strained, and it seems likely that there are barriers to the ring closure reactions of 7 to 9 and 10. All of these arguments support the hypothesis that 7 would lie in an absolute potential energy minimum and could thus be characterizable under appropriate experimental conditions.

REFERENCES FOR CHAPTER 1.

1. Berson, J. A. Accts. Chem. Res., 1978, 11, 446-453.
2. Gajewski, J. J. "Hydrocarbon Thermal Isomerizations", Academic Press, New York, 1980.
3. Wagner, P. J. in "Rearrangements in Ground and Excited States", de Mayo, P., Ed., Academic Press, New York, 1980.
4. Michl, J., Ed. Tetrahedron, 1982, 38, 733-868.
5. Borden, W. T., Ed. "Diradicals", Wiley, New York, 1982.
6. Berson, J. A. in reference 5, p. 151-194, and references therein.
7. Kelley, D. F.; Rentzepis, P. M.; Mazur, M. R. and Berson, J. A. J. Am. Chem. Soc., 1982, 104, 3764-3766.
8. Buchwalter, S. L. and Closs, G. L. J. Am. Chem. Soc., 1979, 101, 4688-4694.
9. Simmons, H. E. and Fukunaga, T. J. Am. Chem. Soc., 1957, 89, 5208-5215. Hoffmann, R.; Imamura, A. and Zeiss, G. D. Ibid., 1967, 89, 5215-5220. Duerr, H. and Gleiter, R. Angew. Chem. Int. Ed. Engl., 1978, 17, 559-569.
10. Batich, C.; Heilbronner, E.; Rommel, E.; Semmelhack, M. F. and Foos, J. S. J. Am. Chem. Soc., 1974, 96, 7662-7668.
11. Hill, R. K.; Morton, G. H.; Rogers, D. W. and Choi, L. S. J. Org. Chem., 1980, 45, 5163-5166.
12. Schweig, A.; Weidner, U.; Hill, R. K. and Cullison, D. A. J. Am. Chem. Soc., 1973, 95, 5426-5427.

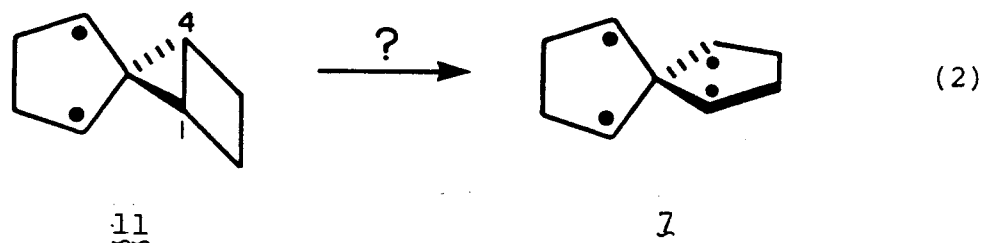
13. Goldberg, A. H. and Dougherty, D. A. J. Am. Chem. Soc., 1983, 105, 284-290.
14. Salem, L. and Rowland, C. Angew. Chem. Int. Ed. Engl., 1972, 11, 92-111.
15. Greenberg, A. and Liebman, J. F. "Strained Organic Molecules", Academic Press, New York, 1978, (a) p. 72, (b) p. 83.
16. Dewar, M. J. S. and Thiel, W. J. Am. Chem. Soc., 1977, 99, 4899-4907, 4907-4917.
17. Bigot, B.; Devaquet, A. and Turro, N. J. J. Am. Chem. Soc., 1981, 103, 6-12.

CHAPTER II

Theoretical Studies on  
1,4,6,9-Spiro[4.4]nonatetrayl

A. MNDO Study of the Ring Opening of Bicyclo[2.1.0]pentanes

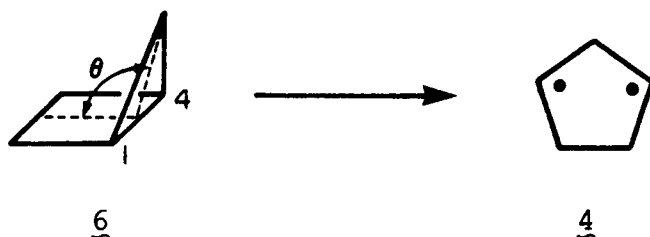
One of the pathways considered for generating 7 was the ring opening of biradical 11. Cleavage of the C1-C4 bond would release ca. 50 kcal/mol of strain energy and allow the full spiroconjugative stabilization of 7 to develop. Thus, if 7 were to benefit sufficiently from this stabilization, the novel biradical-to-tetraradical rearrangement of eq. 2 would be feasible.



A computational estimate of the viability of eq. 2 was desired and an ab initio investigation of the pathway would be prohibitively expensive. It was thus decided to study the conversion of 11 to 7 using the semi-empirical computational method MNDO<sup>1</sup> despite uncertainties associated with the application of this method to structures containing three and four membered rings. It must also be considered that due to lack of correlation of the non-bonded electrons, the single determinant MNDO wavefunction does not provide an entirely accurate description of the electronic states of singlet biradicals. However, it was possible that large spiroconjugative effects on the ring opening of 11 would be

detected if calculations on 11  $\rightarrow$  7 were compared to a model system in which spiroconjugation is not possible.

For purposes of comparison, the ring opening of bicyclo[2.1.0]pentane (6) to 1,3-cyclopentadiyl (4) was first studied. The structures were constrained to be singlets



of  $C_s$  symmetry as the angle  $\theta$  was opened in 10 degree increments from 117 to 177°. At each point the geometry was optimized with the C-H, C1-C2 (= C4-C3 by symmetry), and C2-C3 bond lengths held constant. Results of the calculations are presented in Table I. It is clear that the activation energy for the ring opening is overestimated since the activation energy for isomerization (bridge-flip) in endo-2-methylbicyclo[2.1.0]pentane is 39.2 kcal/mole.<sup>2</sup> This discrepancy is to be expected as the single determinant wavefunction would be lowered considerably in energy by configuration interaction.

Calculations on 11 began with a geometry constructed from the MNDO-optimized structure of 6 and Schaefer's geometry for 4.<sup>3</sup> The molecule was restricted to a triplet spin state and  $C_s$  symmetry while the parameters for geometry optimization were varied as for 6. As can be seen in Table II,



TABLE I. MNDO Heats of Formation for Points along the Conversion of 6 to 4.

$\theta$ (deg)	$\Delta H_f^\circ$ (kcal/mol)	$\Delta(\Delta H_f)$ (kcal/mol)	C1-C4 Bond Length ( $\text{\AA}$ )
117.29	30.78		1.554
127.29	34.01	3.23	1.571
137.29	43.19	12.40	1.594
147.29	57.26	26.45	1.628
157.29	74.75	43.96	1.748
167.29	77.16	46.38	2.221
177.29	78.23	47.45	2.254

TABLE II. MNDO Heats of Formation for Points along the Conversion of 11 to 7.

$\theta$ (deg)	$\Delta H_f^\circ$ (kcal/mol)	$\Delta(\Delta H_f)$ (kcal/mol)	C1-C4 Bond Length (Å)
117.29	76.44		1.543
122.29	76.49	0.05	1.555
127.29	78.51	2.07	1.560
132.29	82.26	5.82	1.573
137.29	87.59	11.15	1.579
147.29	102.23	25.79	1.601
157.29	121.07	44.63	1.657
167.29	130.89	54.45	2.144

MNDO predicts a higher activation energy for  $\underline{11} \rightarrow \underline{7}$  than for  $\underline{6} \rightarrow \underline{4}$ . Examination of the MNDO orbitals for  $\underline{11}$  ( $\theta=167^\circ$ ) reveals that the low symmetry of the structure prevents effective mixing of the non-bonding orbitals. In addition, the MNDO wavefunction provides no means for correlation of the four radical electrons. It is not surprising that the wavefunction for  $\underline{7}$  with four badly correlated electrons leads to a higher activation energy for ring opening of  $\underline{11}$  than is calculated for  $\underline{6}$ , in which the wavefunction is inadequately described for only two electrons. It seems that the economically feasible semi-empirical calculations are inappropriate for the system and that these results provide no useful information.

#### B. Qualitative Molecular Orbital Analysis of Spirononatetrayl. The Biradical Model.

A short discussion of the electronic structure of tetraradical  $\underline{7}$  as predicted by MO theory has been presented in Chapter I, and it will be expanded here. The magnitude of the predicted  $b_1-a_2$  split in  $\underline{7}$  suggests the orbital occupation shown in Figure 1. This  $b_1^2 e^2$  configuration, at the level of one-electron theory, implies a substantial stabilization as compared to a tetraradical in which the four radical centers do not interact (four electrons in four NBMO). Thus, a major goal of the present work has been to determine the extent to which the  $b_1^2 e^2$  configuration of Figure 1 correctly describes the electronic structure of  $\underline{7}$ .

This biradical configuration gives rise to four states: a triplet and three singlets.<sup>4</sup> These states are as shown in eq. 3-6. Both  $^1A_1$  and  $^1B_2$  have zwitterionic character, and are expected to be higher lying in energy. The  $^3A_2$  and  $^1B_1$  states are both pure biradical or covalent states, and at the level of two-electron theory, one would predict an energetic ordering of  $^3A_2 < ^1B_1$ , due to the exchange repulsions in the singlet.

$$^3A_2 = \frac{1}{\sqrt{2}}A[(\dots b_1^2 e_x e_y) - (\dots b_1^2 e_y e_x)](\alpha\beta + \beta\alpha) \quad (3)$$

$$^1B_1 = \frac{1}{\sqrt{2}}A[(\dots b_1^2 e_x^2) - (\dots b_1^2 e_y^2)](\alpha\beta - \beta\alpha) \quad (4)$$

$$^1A_1 = \frac{1}{\sqrt{2}}A[(\dots b_1^2 e_x^2) + (\dots b_1^2 e_y^2)](\alpha\beta - \beta\alpha) \quad (5)$$

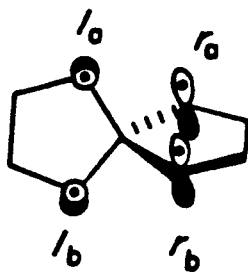
$$^1B_2 = \frac{1}{\sqrt{2}}A[(\dots b_1^2 e_x e_y) + (\dots b_1^2 e_y e_x)](\alpha\beta - \beta\alpha) \quad (6)$$

However, one can anticipate that configuration interaction (CI) will preferentially stabilize the singlet and lead to a  $^1B_1 < ^3A_2$  energetic ordering. This prediction is based on analogy to square ( $D_{4h}$ ) cyclobutadiene, for which 7 is a three-dimensional analogue. In cyclobutadiene, the electronic configuration analogous to that of Figure 1 gives rise to the same four states as in eq. 3-6, with the symmetry

labels augmented by a subscript g.<sup>5</sup> Thus,  $^1A_{1g}$  and  $^1B_{2g}$  are high-lying, zwitterionic states. Since the NBMO of cyclobutadiene can be confined to disjoint sets of atoms, exchange repulsions in the  $^1B_{1g}$  state are minimal.<sup>6</sup> When CI is included in the wavefunction,  $^1B_{1g}$  is preferentially stabilized and emerges as the ground state, with  $^3A_{2g}$  slightly higher.<sup>7</sup> Clearly, the NBMO of Figure 1 span disjoint sets of atoms, and one would expect minimal exchange repulsions in the  $^1B_1$  state of 1. Thus, qualitative MO considerations predict a singlet ground state for 1 ( $^1B_1$ ) with a low-lying  $^3A_2$  state.

C. Qualitative Valence Bond Analysis of Spiroonatotetrayl.  
The Tetraradical Model.

Valence bond theory presents an alternative model for the electronic interactions in 1. In this view, 1 is considered as essentially a tetraradical with little spiro-conjugation. The electronic structure of such a species can be analyzed in terms of valence bond (VB) wavefunctions, in which there is one electron in the nonbonding p orbital of each of the four radical carbons. Labeling these orbitals as  $l_a$  and  $l_b$  on the left diyl and  $r_a$  and  $r_b$  on the right diyl, as in 12



leads to a singlet state (eq. 7) and a triplet state (eq. 8)

$${}^1\Psi_z = (z_a z_b + z_b z_a)(\alpha\beta - \beta\alpha) \quad (7)$$

$${}^3\Psi_z = (z_a z_b - z_b z_a) \begin{Bmatrix} (\alpha\alpha) \\ (\alpha\beta + \beta\alpha) \\ (\beta\beta) \end{Bmatrix} \quad (8)$$

on the left and similar wavefunctions  ${}^1\Psi_r$  and  ${}^3\Psi_r$  on the right. In the VB model the total wavefunction of the tetraradical is formed by products of these wavefunctions, leading to the combinations of eq. 9.

$$\text{SS: } {}^1\Psi_z(1,2) {}^1\Psi_r(3,4)$$

$$\text{TS} \pm \text{ST: } {}^3\Psi_z(1,2) {}^1\Psi_r(3,4) \pm {}^1\Psi_z(1,2) {}^3\Psi_r(3,4) \quad (9)$$

$$\text{TT: } {}^3\Psi_z(1,2) {}^3\Psi_r(3,4)$$

Antisymmetrization, to satisfy the Pauli principle, and consideration of the  $D_{2d}$  symmetry of the system lead to the wavefunctions in eq. 10-14.

$$\text{SS} = {}^1A_1 = A\{z_a z_b r_a r_b [(\alpha\beta - \beta\alpha)(\alpha\beta - \beta\alpha)]\} \quad (10)$$

$$(\text{TS} \pm \text{ST}) = {}^3E = A\{z_a z_b r_a r_b [\alpha\alpha(\alpha\beta - \beta\alpha) \pm (\alpha\beta - \beta\alpha)\alpha\alpha]\} \quad (11)$$

$$^1_{TT} = ^1_{B_1} = A\{l_a l_b r_a r_b [\alpha\alpha\beta\beta + \beta\beta\alpha\alpha - \frac{1}{2}(\alpha\beta + \beta\alpha)(\alpha\beta + \beta\alpha)]\} \quad (12)$$

$$^3_{TT} = ^3_{A_2} = A\{l_a l_b r_a r_b [\alpha\alpha(\alpha\beta + \beta\alpha) - (\alpha\beta + \beta\alpha)\alpha\alpha]\} \quad (13)$$

$$^5_{TT} = ^5_{B_1} = A\{l_a l_b r_a r_b [\alpha\alpha\alpha\alpha]\} \quad (14)$$

The TT cases bear some discussion here. With a pair of two-electron triplets, there is a total of  $3 \times 3 = 9$  states. However, resolving these states in terms of the total spin for the four-electron system leads to total spins of  $S=2$ , 1, and 0, i.e., a quintet ( $^5B_1$ ), a triplet ( $^3A_2$ ) and a singlet ( $^1B_1$ ), for a total of nine states. In the approximation that the two triplets interact only weakly, the three TT states can be described by a Heisenberg Hamiltonian<sup>8</sup> (eq. 15),

$$E_s = E_0 + JS(S + 1), \quad (15)$$

where  $J$  is the exchange coupling term. In the case that the orbitals of the two T states overlap, the  $J$  is expected to be positive, so that  $^1B_1$  is lowest in energy. The energies of the higher spin states are then as in eq. 16,

$$\begin{aligned} E(^3A_2) &= E(^1B_1) + 2J \\ E(^5B_1) &= E(^1B_1) + 6J \end{aligned} \quad (16)$$

In the case that the  $l$  and  $r$  orbitals are orthogonal, eq. 16 still applies, but  $J$  will be negative, leading to a quintet ground state.

Assuming *no* interaction of the two 1,3-cyclopentanediy1 fragments, one would expect the intrinsic 0.9 kcal/mol preference calculated for the triplet state in this fragment<sup>3,9</sup> to generate the energy spectrum of eq. 17.

$$E(SS) = (E(TS) + 0.9) = (E(TT) + 1.8) \quad (17)$$

Summarizing the VB description, a tetraradical is expected to have six low-lying, covalent (non-ionic) states: two singlets, three triplets, and a quintet. The closeness of these six states is the signature of a tetraradical.

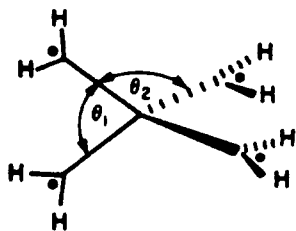
#### D. Ab Initio Computational Methods

Unless otherwise noted, all calculations were performed with a valence double-zeta (VDZ) basis set. Dunning's contraction<sup>10</sup> (3s, 2p) of Huzinaga's (9s, 5p) basis set<sup>11</sup> was used for carbon, and for hydrogen a comparable (4s/2s) contraction with each Gaussian exponent scaled by a factor of 1.44 was employed.<sup>10</sup> In those cases where carbon polarization functions were included, the orbital exponent was 0.75. All C-C bond lengths were 1.52 Å, in accord with Schaefer's geometry optimization<sup>3</sup> of the triplet state of 4, and all C-H bond lengths were 1.09 Å. Hartree-Fock calculations were performed using the MQM:GVB2P5 program.<sup>12</sup>



The configuration interaction (CI) calculations were carried out using the MQM:CI2P5 program.<sup>13</sup> Multiconfiguration self-consistent field (MCSCF) calculations utilized the MQM:GVB3 program.<sup>14</sup>

All ab initio calculations were performed on the model system tetramethylenemethane. Several recent studies have demonstrated that deleting the ethano bridges in 1,3-cyclopentanediy1 (4) and related structures such as 1 does not significantly alter the electronic structures of the molecules,<sup>9,15</sup> thus verifying the validity of this model. For most calculations a  $D_{2d}$  structure (13) was considered, with different sets of C-C-C angles. In 13a, the central carbon is tetrahedral giving a structure which is unbiased with respect to favoring or disfavoring the spiroconjugative effect. In 13b,  $\theta_1 = 102^\circ$ , which is the value calculated by Schaefer<sup>3</sup> for the analogous angle in 4. Thus, 13a may be considered a general model for the electronic interactions we intend to study, while 13b is perhaps a better model for the precise interactions present in structure 7.



	$\theta_1$	$\theta_2$
a	109.5	109.5
b	102.0	113.3

13

## E. Results and Discussion for Ab Initio Studies on Spiroononatetrayl

Spiroconjugation. As a test for the effectiveness of spiroconjugation in 7, the Hartree-Fock (HF) wavefunctions were determined for the  $^5B_1$  states of 13a and 13b. These quintet states do indeed possess MO's like those of Figure 1, and the  $b_1$ - $a_2$  energy gap is 2.71 eV in 13a and 2.25 eV in 13b. Thus, the qualitative prediction of a significant  $b_1$ - $a_2$  split in 7 is confirmed, and the magnitude is roughly as expected. Note that the value for 13b, whose geometry closely approximates that expected for the spiro-[4.4]nonane ring system, is very nearly the 1.96 eV predicted from Schweig's empirical formula (eq. 1). Clearly, the smaller value of  $\theta_1$  in 13b moves the spiroconjugatively interacting radical centers further apart and thus diminishes the orbital splitting relative to 13a.

Electronic States of 13a. One of the major goals of this work has been to determine the ground electronic state for a structure such as 7 and the nature of any other low-lying states. The number of low-lying states (two for a biradical, six for a tetraradical) would indicate the fundamental electronic structure of 7 and allow the more appropriate of the MO and VB models to be chosen. The first step was allowing a complete CI for 13a within the space of the  $b_1$ ,  $e$  and  $a_2$  orbitals using the MO's determined in the HF calculation on  $^5B_1$  and the VDZ basis set (CI-VDZ). This resulted in six low-lying states energetically ordered

as:  ${}^1B_1 < {}^3A_2 < {}^3E < {}^1A_1 < {}^5B_1$ . The relative energies are given in Table III, and the contributions of the various configurations to these states is given in Table IV. There is a >6 eV energy gap between these six states and the next lowest state. Energies of higher lying states can be found in Table V.

In order to evaluate the reliability of the CI wavefunctions in predicting the relative energies of these states, the calculations on 13a were extended in several ways, as summarized in Table III. Determination of the multiconfiguration self-consistent field (MCSCF) wavefunctions (equivalent to full GVB wavefunctions<sup>16</sup>) for 13a with the VDZ basis set for the singlet and triplet states led to only a minor decrease in energy relative to the CI wavefunctions. Similarly, repeating the CI calculations with the VDZ basis set augmented by a set of polarization functions (d orbitals) on each carbon (CI+d) led to only a minor change in relative energies. Finally, starting with the  ${}^1B_1$  MCSCF-VDZ wavefunction and allowing a full CI within the  $b_1$  e  $a_2$  space plus all single and double excitations from these orbitals into the virtual orbitals (POL(4/2)) stabilized the  ${}^1B_1$  state by only 2.55 kcal/mol relative to the MCSCF  ${}^1B_1$  wavefunction. By comparison, the corresponding POL(2/2) calculation on the  ${}^5B_1$  state led to a 1.03 kcal/mol stabilization relative to the HF wavefunction.

TABLE III. Relative Energies (kcal/mol) for Covalent States of 13.

	Geometry 13a				Geometry 13b
	CI-VDZ <sup>b</sup>	MCSCF <sup>c</sup>	CI+d <sup>d</sup>	RCI <sup>e</sup>	CI-VDZ <sup>f</sup>
<sup>1</sup> B <sub>1</sub> (TT)	-8.51	-10.12	-9.92	+7.61	-3.51
<sup>3</sup> A <sub>2</sub> (TT)	-6.56	- 7.31	-7.61	+5.06	-2.90
<sup>3</sup> E (TS)	-2.44	- 3.22	-2.99	+3.45	-1.11
<sup>1</sup> A <sub>1</sub> (SS)	-2.08	- 2.60	-2.71	+4.35	-0.92
<sup>5</sup> B <sub>1</sub> (TT)	0.00 <sup>a</sup>	0.00	0.00	0.00	0.00

<sup>a</sup>Total Energy: -193.73288 h

<sup>b</sup>Full four electron CI within the b<sub>1</sub>, e, a<sub>2</sub> space using the orbitals from the HF solution on the <sup>5</sup>B<sub>1</sub> state. Total energy of the <sup>1</sup>B<sub>1</sub> state: -193.74644 h.

<sup>c</sup>Full MCSCF solutions for each state using all configurations for four electrons distributed over the b<sub>1</sub>, e, a<sub>2</sub> space. Total energy of the <sup>1</sup>B<sub>1</sub> state: -193.74902 h.

<sup>d</sup>Same solutions as in b except that d functions were included on all carbons. Total energy of the <sup>1</sup>B<sub>1</sub> state: -193.81752 h.

<sup>e</sup>Four electron CI within the r<sub>+</sub>r<sub>-</sub>l<sub>+</sub>l<sub>-</sub> space, using the partially localized orbitals of Figure 3 obtained through linear combinations of the orbitals from the HF solution for <sup>5</sup>B<sub>1</sub>. Configurations restricted to those of the (r<sub>+</sub>r<sub>-</sub>)<sup>2</sup>(l<sub>+</sub>l<sub>-</sub>)<sup>2</sup> type. Total energy of the <sup>1</sup>B<sub>1</sub> state: -193.72074 h.

<sup>f</sup>Same solutions as in b except for the geometry. Total energy of <sup>1</sup>B<sub>1</sub>: -193.73124 h.

TABLE IV. CI-VDZ Wavefunctions for Covalent States of 13a.

State	Configuration				Coeff. <sup>a</sup>
	$b_1$	$e_x$	$e_y$	$a_2$	
$^1B_1$	2	0	2	0	-.55
	2	2	0	0	.55
	1	1	1	1	-.47
	0	0	2	2	.30
	0	2	0	2	-.30
$^3A_2$	2	1	1	0	.67
	1	0	2	1	.46
	1	2	0	1	-.46
	0	1	1	2	-.36
$^3E^b$	1	1	2	0	.59
	2	0	1	1	.56
	0	2	1	1	-.42
	1	1	0	2	-.40
$^1A_1$	0	2	2	0	.51
	1	1	1	1	-.48
	2	0	0	2	.46
	2	2	0	0	-.35
	2	0	2	0	-.35
	0	2	0	2	-.17
	0	0	2	2	-.17
$^5B_1$	1	1	1	1	1.0

<sup>a</sup>Only configurations with coefficients greater than 0.05 are included.

<sup>b</sup>The other component of  $^3E$  is not shown. To obtain it, interchange the occupations of  $e_x$  and  $e_y$ .

TABLE V. Relative Energies (eV) for States of 13.<sup>f</sup>

	Geometry 13a				Geometry 13b
	CI-VDZ <sup>a</sup>	MCSCF <sup>b</sup>	CI+d <sup>c</sup>	RCI <sup>d</sup>	CI-VDZ <sup>e</sup>
<sup>1</sup> B <sub>1</sub>	0.000	0.000	0.000	0.000	0.000
<sup>3</sup> A <sub>2</sub>	0.084	0.119	0.100	-0.111	0.026
<sup>3</sup> E	0.263	0.299	0.301	-0.181	0.104
<sup>1</sup> A <sub>1</sub>	0.279	0.326	0.313	-0.142	0.112
<sup>5</sup> B <sub>1</sub>	0.369	0.439	0.430	-0.330	0.152
<sup>1</sup> B <sub>2</sub>	6.727		6.593		6.768
<sup>1</sup> E	7.960		7.813		7.620
<sup>3</sup> E	7.967		7.848		7.839
<sup>3</sup> A <sub>2</sub>	7.976		7.844		7.848
<sup>1</sup> A <sub>1</sub>	8.273		8.184		7.987
<sup>3</sup> A <sub>1</sub>	8.641		8.612		8.345
<sup>3</sup> B <sub>2</sub>	8.818		8.781		8.539
<sup>1</sup> E	9.268		9.212		9.298
<sup>3</sup> B <sub>1</sub>	9.436		9.331		9.021
<sup>3</sup> E	9.534		9.478		9.069
<sup>1</sup> A <sub>1</sub>	9.905		9.860		9.528
<sup>1</sup> A <sub>2</sub>	10.127		10.023		10.016
<sup>3</sup> B <sub>1</sub>	10.229		10.163		9.991
<sup>1</sup> B <sub>1</sub>	10.594		10.538		10.341

TABLE V. (Cont'd).

	CI-VDZ <sup>a</sup>	MCSCF <sup>b</sup>	CI+d <sup>c</sup>	RCI <sup>d</sup>	CI-VDZ <sup>e</sup>
<sup>1</sup> E	11.159		11.145		10.563
<sup>3</sup> E	11.166		11.176		10.780
<sup>1</sup> B <sub>2</sub>	11.281		11.270		10.625
<sup>1</sup> A <sub>1</sub>	17.800		17.669		17.913
<sup>1</sup> B <sub>2</sub>	17.980		17.881		18.200
<sup>1</sup> A <sub>1</sub>	19.219		19.031		18.309
<sup>1</sup> E	19.238		19.050		18.343

<sup>a</sup>Full four electron CI within the  $b_1, e, a_2$  space using the orbitals from the HF solution on the <sup>5</sup>B<sub>1</sub> state. Total energy of the <sup>1</sup>B<sub>1</sub> state: -193.74644 h.

<sup>b</sup>Full MCSCF solutions for each state using all configurations for four electrons distributed over the  $b_1, e, a_2$  space. Total energy of the <sup>1</sup>B<sub>1</sub> state: -193.74902 h.

<sup>c</sup>Same solutions as in a except that d functions were included on all carbons. Total energy of the <sup>1</sup>B<sub>1</sub> state: -193.81752 h.

<sup>d</sup>Four electron CI within the  $r_+r_-l_+l_-$  space, using the partially localized orbitals of Figure 3 obtained through linear combinations of the orbitals from the HF solution for <sup>5</sup>B<sub>1</sub>. Configurations restricted to those of the  $(r_+r_-)^2(l_+l_-)^2$  type. Total energy of the <sup>1</sup>B<sub>1</sub> state: -193.72074 h.

<sup>e</sup>Same solutions as in a except for the geometry. Total energy of <sup>1</sup>B<sub>1</sub>: -193.73124 h.

<sup>f</sup>The highest energy triplet (<sup>3</sup>A<sub>2</sub>) and the highest energy singlet (<sup>1</sup>B<sub>1</sub>) are not shown.

It is thus concluded that the CI-VDZ wavefunction using the HF  ${}^5B_1$  orbitals provides a good description of the electronic structure of 13a and subsequent discussions will emphasize this level of theory. For a best estimate of the  ${}^1B_1$ - ${}^5B_1$  energy gap, one might assume that the stabilizations afforded  ${}^1B_1$  by the various extensions of the CI-VDZ wavefunctions are additive.<sup>17</sup> This leads to a value of  $8.5 + 1.4$  (d-orbitals) +  $1.6$  (MCSCF) +  $1.5$  (POL4/2) =  $13.0$  kcal/mol.

The CI wavefunctions for 13a have also been determined using the set of partially localized orbitals of Figure 3. Each localized orbital is confined to one "ring", i.e., a trimethylene unit that models a five-membered ring in 7, and the orbitals are designated r or l according to whether they derive from the right or left ring. The subscript describes the phase relationship between the p orbitals. The resulting wavefunctions, shown in Table VI, allow one to confirm that the six low-lying states for 13a do, indeed, correspond to the six covalent states discussed above (eq. 10-14). For each state, each ring is in either a biradical singlet or a triplet state in the dominant configurations. The  ${}^1B_1$  ground state is dominated by a (1111) configuration, and the spin eigenfunction is the coupling of two triplets to give an overall singlet.<sup>18</sup> Its triplet counterpart is  ${}^3A_2$ , also with a (1111) spatial configuration, but possessing spin eigenfunctions representing two ring triplets coupled to an overall triplet



FIGURE 3. Partially Localized Orbitals of 13a.

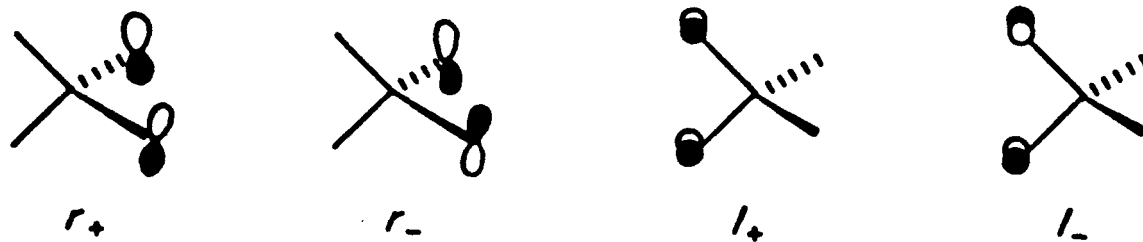


TABLE VI. CI-VDZ Wavefunctions of 13a Using the Partially Localized Orbitals of Figure 3.

State	Configuration				Coeff. <sup>a</sup>
	$r_+$	$r_-$	$l_+$	$l_-$	
$1B_1$	1	1	1	$1^b$	.97
	1	2	1	0	-.18
	1	0	1	2	-.18
$3A_2$	1	1	1	$1^c$	-.77
	1	1	1	$1^d$	.59
	1	2	1	0	.16
	1	0	1	2	.16
$3E^e$	2	0	1	1	.50
	1	1	2	0	.50
	0	2	1	1	-.48
	1	1	0	2	-.48
	2	1	1	0	.09
	1	0	2	1	-.09
	0	1	1	2	.08
	1	2	0	1	-.08
$1A_1$	0	2	2	0	.50
	2	0	0	2	.50
	2	0	2	0	-.51
	0	2	0	2	-.46
	0	1	2	1	-.13
	2	1	0	1	-.13
$5B_1$	1	1	1	1	1.00

<sup>a</sup>Only configurations with coefficients greater than 0.05 are included.

<sup>b</sup>Spin Eigenfunction:  $A\{r_+r_-l_+l_-[\alpha\alpha\beta\beta+\beta\beta\alpha\alpha-1/2(\alpha\beta+\beta\alpha)(\alpha\beta+\beta\alpha)]\}$

<sup>c</sup>Spin Eigenfunction:  $A\{r_+r_-l_+l_-[\alpha\alpha\beta\alpha-1/2(\alpha\beta+\beta\alpha)\alpha\alpha]\}$

<sup>d</sup>Spin Eigenfunction:  $A\{r_+r_-l_+l_-[\alpha\alpha\alpha\beta-1/3(\alpha\alpha\beta+\alpha\beta\alpha+\beta\alpha\alpha)\alpha]\}$

<sup>e</sup>The other component of  $3E$  is not shown. To obtain it, interchange the occupations of the left and right ring components.

wavefunction. The  ${}^5B_1$  state is straightforward, as the (1111) configuration is required in the high spin case. The other states contain biradical singlets, as evidenced by the fact that each configuration containing a doubly occupied orbital is accompanied by an out-of-phase mixture<sup>19</sup> of the configuration with the alternative orbital of the same ring doubly occupied. For example, a  $r_+^2 r_-^0 (1_+ 1_-)^2$  configuration is always paired out-of-phase with the analogous  $r_+^0 r_-^2 (1_+ 1_-)^2$  configuration.

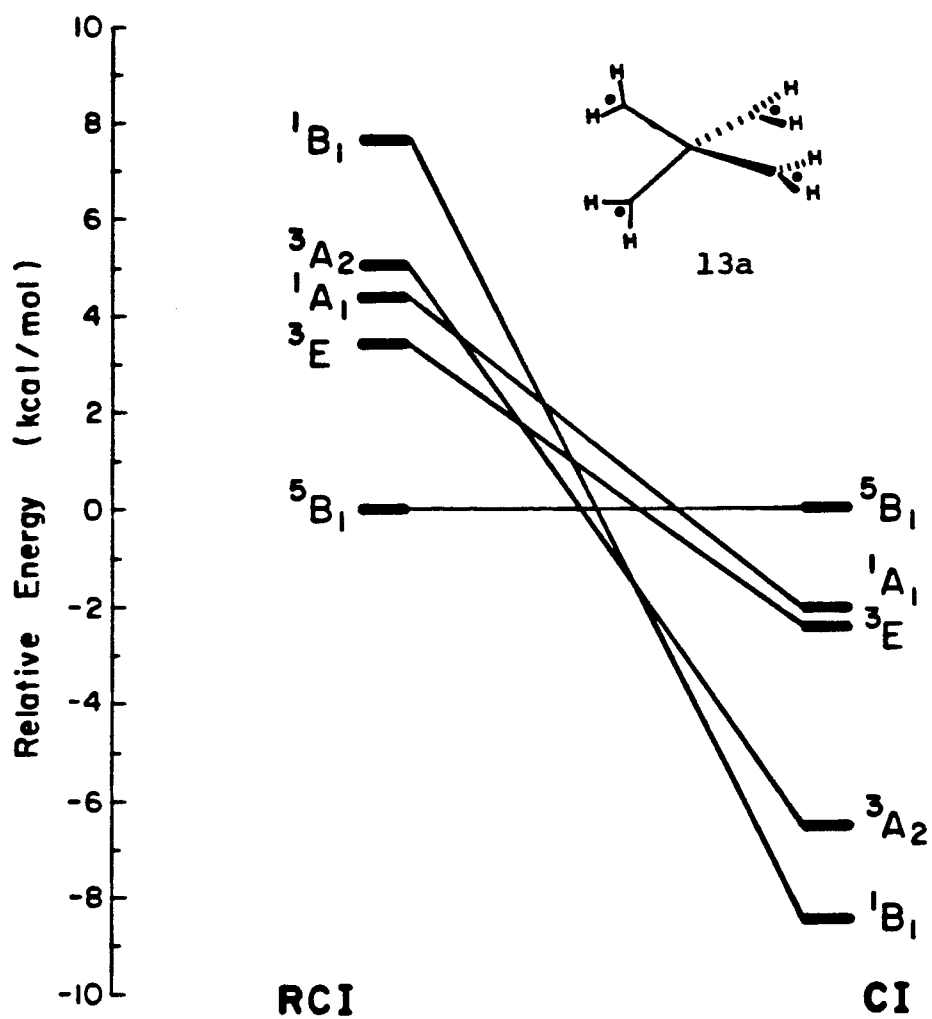
As can be seen in Table V, in the singlet manifold, after  ${}^1B_1$  and  ${}^1A_1$ , there is a substantial energy gap to a collection of states with excitation energies in the range 6.7 to 11.3 eV (CI-VDZ). Inspection of these states using the localized orbitals reveals that each contains one ring in a biradical singlet state and one ring in a zwitterionic state. There is then another gap to a group of states with excitation energies from 17.8 to 19.2 eV, for which both rings have zwitterionic character. In the triplet manifold, all higher states fall in the range of 7.9 to 11.1 eV, since there can be no doubly zwitterionic states. The total number of higher-lying singlets is eighteen, while there are twelve higher-lying triplets. Combined with the six low-lying covalent states this produces the 36 states one expects from placing four electrons in four orbitals.

The results for 13a clearly indicate that the electronic structure of 7 is essentially that of a tetraradical, and not a biradical. There are six low-lying states, and not two as

predicted for a biradical. However, the results also demonstrate a significant interaction across the two five-membered rings, i.e., spiroconjugation. This is seen in the relative energies of the TT states, for which the non-interacting model predicts  ${}^5B_1 < {}^3A_2 < {}^1B_1$ . For 13a, precisely the opposite energetic ordering is seen.

In order to better quantify the spiroconjugative effect, a model for 7 in which spiroconjugation is "turned off" was studied. A CI calculation (VDZ basis) using the localized orbitals of 13a (Figure 3) was performed. However, in the CI double occupation of each ring was forced so that each contained a fully correlated singlet or triplet biradical, but any kind of interaction between the rings was not possible. The results of these restricted CI (RCI) calculations are shown in Table III and Figure 4. There is a dramatic reversal in the order of states in the RCI results relative to the full CI. Analysis reveals that the RCI model shows excellent quantitative agreement with the previously discussed model (eq. 15) assuming orthogonal  $l$  and  $r$  orbitals. The energetic relationships of the TT states summarized in eq. 16 are completely in accord with the RCI results. Considering the  ${}^1B_1$ - ${}^3A_2$  gap leads to a value of -1.28 kcal/mol for  $J$ , while the  ${}^1B_1$ - ${}^5B_1$  gap implies a  $J$  of -1.27 kcal/mol, in stunning agreement. Also, the energy gap between the TS states ( ${}^3E$ ) and the multiplicity-weighted average of the TT states is 0.92 kcal/mol, while that between the TS and SS ( ${}^1A_1$ ) states is 0.90 kcal/mol.

FIGURE 4. Relative Energies of the States of 13a from RCI and CI-VDZ Calculations.



Again, this result is in remarkable agreement with the energy spectrum of eq. 17. Thus, the RCI calculation provides an excellent model for a structure such as 7, but with orthogonal l and r rings.

The results shown in Figure 4 indicate that although spiroconjugation in 13a is not strong enough to turn the tetraradical into a biradical, it does profoundly affect the energetic ordering of the six tetraradical states. In order to rationalize the relative energies of all six states, one must invoke an interplay between two effects. These are the exchange coupling term,  $J$ , of eq. 16, which is an indication of spiroconjugation, and the intrinsic, high-spin preference of the biradical components, summarized in eq. 17. The energetic ordering of the TT states,  $^1B_1 < ^3A_2 < ^5B_1$ , is qualitatively understandable in terms of eq. 16. The energetic ordering  $^3E < ^1A_1$  is consistent with the expectation  $TS < SS$ . Apparently, the  $6J$  destabilization of the  $^5B_1$  state (eq. 16) is enough to lift this TT state above the TS and SS states.

It should be noted that although the qualitative MO model did not suggest the presence of six low-lying states for 13a, it does satisfactorily rationalize the relative energies of these states. The basic consideration in such an analysis is the stabilization of the  $b_1$  MO and the destabilization of the  $a_2$  MO (Figure 1). The clearcut prediction of a  $^1B_1$  ground state followed closely by  $^3A_2$  discussed above is fully confirmed by the calculations.

These states are low-lying because they can fully benefit from the  $(b_1^2 e^2)$  configurations. The  ${}^5B_1$  state is highest in energy because the  $(b_1^1 e_x^1 e_y^1 a_2^1)$  configuration is mandated and does not benefit from the spiroconjugative stabilization of  $b_1$ . The  ${}^3E$  and  ${}^1A_1$  states are of intermediate energy because each is only partially able to take advantage of the spiroconjugative effect. Each configuration that contributes to  ${}^3E$  must have an odd number of electrons in the  $e$  pair of orbitals. Thus, any configuration with  $b_1$  doubly occupied necessarily has  $a_2$  singly occupied (Table II), which partially cancels the stabilizing effect. For the  ${}^1A_1$  state,  $(b_1^2 e^2)$  configurations are possible (eq. 5). However, these are less favorable, because they must have some ionic character, which is destabilizing. The reason that  ${}^1A_1$  is a low-lying state for 7 is that there are several other configurations with  $A_1$  symmetry that can mix with the  $(b_1^2 e^2)$  configuration so as to diminish the ionic nature of the state. This is not the case for  ${}^1B_2$  (eq. 6), and it thus remains high-lying.

The analogy between 7 and  $D_{4h}$  cyclobutadiene has been mentioned previously. At a comparable level of theory (CI-VDZ), the lowest-lying states for  $D_{4h}$  cyclobutadiene, along with relative energies in kcal/mol, are:  ${}^1B_{1g}$  (0),  ${}^3A_{2g}$  (10),  ${}^1A_{1g}$  (50),  ${}^1B_{2g}$  (84),  ${}^3E_u$  (90) and  ${}^5B_{1g}$  (152).<sup>20</sup> The overall pattern is similar to that for 7, but the energetic advantage of pairing two electrons in the lowest  $\pi$  MO is much greater than that of doubly occupying the  $b_1$

MO of 7. This is why  $^1A_{1g}$  lies well below  $^3E_u$  and why  $^1B_{2g}$  is lower than  $^3E_u$ , even though  $^1B_{2g}$  is not a covalent state.

Electronic States of 13b. On going from 13a to 13b, in which  $\theta_1 = 102^\circ$ , the magnitude of the spiroconjugative effect is diminished, as indicated by the smaller  $b_1$ - $a_2$  gap in the HF  $^5B_1$  orbitals. By coincidence, the singlet-triplet energy gap in (0,0)-trimethylene, the fragment from which 13 is built, is the same whether  $\theta_1 = 102^\circ$  or  $\theta_1 = 109.5^\circ$ .<sup>9</sup> Thus, the intrinsic electronic structure of the fragments is not significantly affected by this angle change. Given this result and the above analysis of 13a, one would expect that distorting 13a to 13b would not alter the energetic ordering of the low-lying states, but would simply diminish the magnitudes of the energy separations. The results shown in Table III confirm this expectation. Thus, all of the above discussion of the electronic structure of 13a is directly applicable to 13b, with the only necessary change being a small weakening of the spiroconjugative effect due to increased distance between the interacting centers.

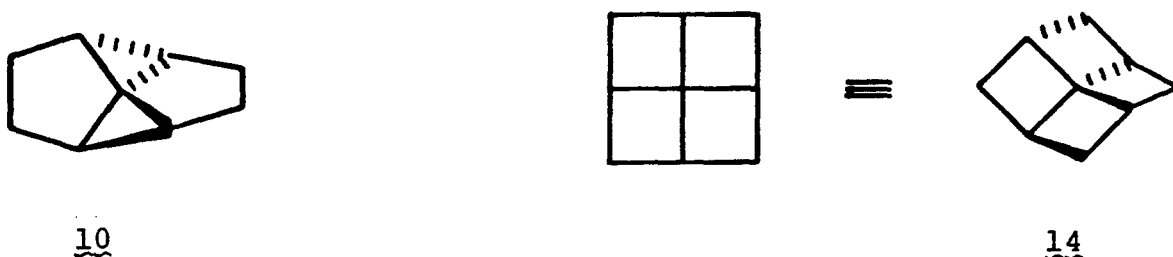
Stabilization of 7. One of the major goals of the present work has been to assess the extent to which spiroconjugation in 7 stabilizes the molecule relative to a "normal" tetraradical. The choice of reference point is crucial to this determination. Given the above discussion it would seem that the RCI description provides a useful



model for what a structure such as 7 would be like if there were no spiroconjugation. One could then say, for example, that  $^1B_1$  is stabilized by  $8.51 + 7.61 = 16.12$  kcal/mol (Table III). For a reference state that models a truly typical tettraradical, it would perhaps be better to consider the spin-multiplicity-weighted average energy of the RCI states, which is 2.99 kcal/mol above the HF  $^5B_1$  state. The  $^1B_1$  stabilization would then be  $8.51 + 2.99 = 11.50$  kcal/mol.

In considering structure 7, one should make two corrections to the above numbers. The RCI-CI comparisons are all based on simple CI-VDZ wavefunctions. It has been shown that including d-orbitals, using an MCSCF wavefunction and allowing excitations into higher orbitals (POL(4/2)) all enhance the magnitude of the spiroconjugative effect slightly. The stabilization energy could be similarly increased, but the overall effect would be relatively small. The second correction concerns the choice of the best geometry to model 7. All of the RCI calculations were based on structure 13a, with  $\theta_1 = 109.5^\circ$ . In 13b, with  $\theta_1$  the same as that calculated for the analogous angle in biradical 4 ( $102^\circ$ ), the spiroconjugative effect is smaller. It seems possible that in 7  $\theta_1$  might expand significantly beyond  $102^\circ$ , at the expense of ring strain, so as to enhance spiroconjugation. However, it still seems likely that in 7,  $\theta_1$  is less than  $109.5^\circ$ , and a stabilization energy based on structure 13a is probably overestimated.

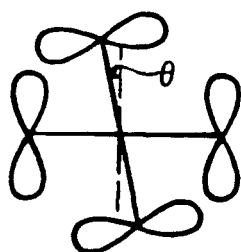
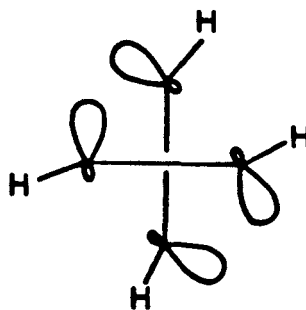
Geometrical Distortions. Given the analogy between 7 and square cyclobutadiene, one might expect a second-order Jahn-Teller distortion of the  $^1B_1$  state, analogous to the stabilizing square-to-rectangular distortion of singlet cyclobutadiene.<sup>7</sup> This would push the molecule toward one of its closed shell forms, tetracyclo[4.3.0.0<sup>1,5</sup>.0<sup>2,9</sup>]nonane (10,  $D_2$  symmetry). Compound 10 could also be called [5.3.5.3]fenestrane, and like its isomer [4.4.4.4]fenestrane (14), 10 should be highly strained, with the spiro carbon distorted toward planarity.<sup>21</sup> In order to get some feeling for the nature of such a structure,



the geometry of 10 was completely optimized using MNDO. As discussed in Chapter I, this semi-empirical method predicts  $\Delta H_f^\circ$  (10 = 110.5 kcal/mol and a strain energy of 139 kcal/mol. It is interesting to compare these results with a recent treatment of 14 at the same level of theory.<sup>22</sup> For 14, MNDO predicts  $\Delta H_f^\circ$  = 150.6 kcal/mol, giving a strain energy of 179 kcal/mol.<sup>22</sup> It can be seen that 10 is predicted to be much less strained than 14. The MNDO geometry of 10 does not contain a planar carbon, although it

is highly strained. The six C-C-C angles around the spiro carbon are pairwise related by symmetry, and have values of  $67.3^\circ$  (internal to cyclopropane),  $126.8^\circ$  (internal to cyclopentane) and  $141.8^\circ$ .

Ab initio theory has been used in two attempts to determine whether 7 will undergo a stabilizing, second-order Jahn-Teller distortion. Structure 15, in which one end of 13a was rotated around the  $S_4$  axis by an angle  $\theta = 10^\circ$  was studied first. The other distortion mode involved a pyramidalization at each carbon in such a way as to produce

1516

structure 16. Such pyramidalization does distort the molecule toward 10, but the carbon atoms are not moved any closer to one another. The pyramidalization was accomplished by moving one hydrogen at each carbon of 13a out-of-plane, such that its C-H bond made a  $30^\circ$  angle with the original C-C-H plane. Both 15 and 16 have  $D_2$  symmetry, which serves to remove all the degeneracies present in 13a.

The results of the calculations on 15 and 16, which were performed at the CI-VDZ level, are summarized in Table VII and Figure 5. Both distortions are destabilizing for 13a, and both lead to only minor perturbations of the relative energies of the six covalent states. It would thus appear that 7 cannot significantly stabilize itself by a second-order Jahn-Teller distortion.

The alternative closed-shell form of 7, 5,5'-spirobis-[bicyclo[2.2.0]pentane], (9,  $C_2$  symmetry) arises by a double disrotatory ring closure of 7. Pursuing the analogy between 7 and cyclobutadiene further, 9 corresponds to tetrahedrane. While the cyclobutadiene-tetrahedrane interconversion is forbidden by orbital symmetry, this is formally not the case for the interconversion of 7 and 9 because of the low symmetry of 9. However, as discussed in Chapter I, 7 - 9 interconversion is forbidden in the sense of the "natural orbital correlations", and one might anticipate a barrier to the double ring closure of 7 to 9.

#### F. Conclusions

The calculations indicate that 7 possesses six low-lying states that correspond to the covalent states of a tetraradical. Thus, the spiroconjugative interaction predicted on the basis of qualitative MO arguments (Figure 1) is not strong enough to convert 7 into a biradical. However, the relative energies of the six tetraradical states are influenced strongly by spiroconjugation.

TABLE VII. Relative Energies (kcal/mol) of the States of 15 and 16.<sup>c</sup>

	<u>15</u> <sup>a</sup>	<u>16</u> <sup>b</sup>
<sup>1</sup> A	3.02	9.36
<sup>3</sup> B <sub>1</sub>	6.19	10.71
<sup>3</sup> B <sub>3</sub>	8.37	13.99
<sup>1</sup> A	11.91	14.59
<sup>3</sup> B <sub>2</sub>	11.96	13.55
<sup>5</sup> A	12.32	14.69

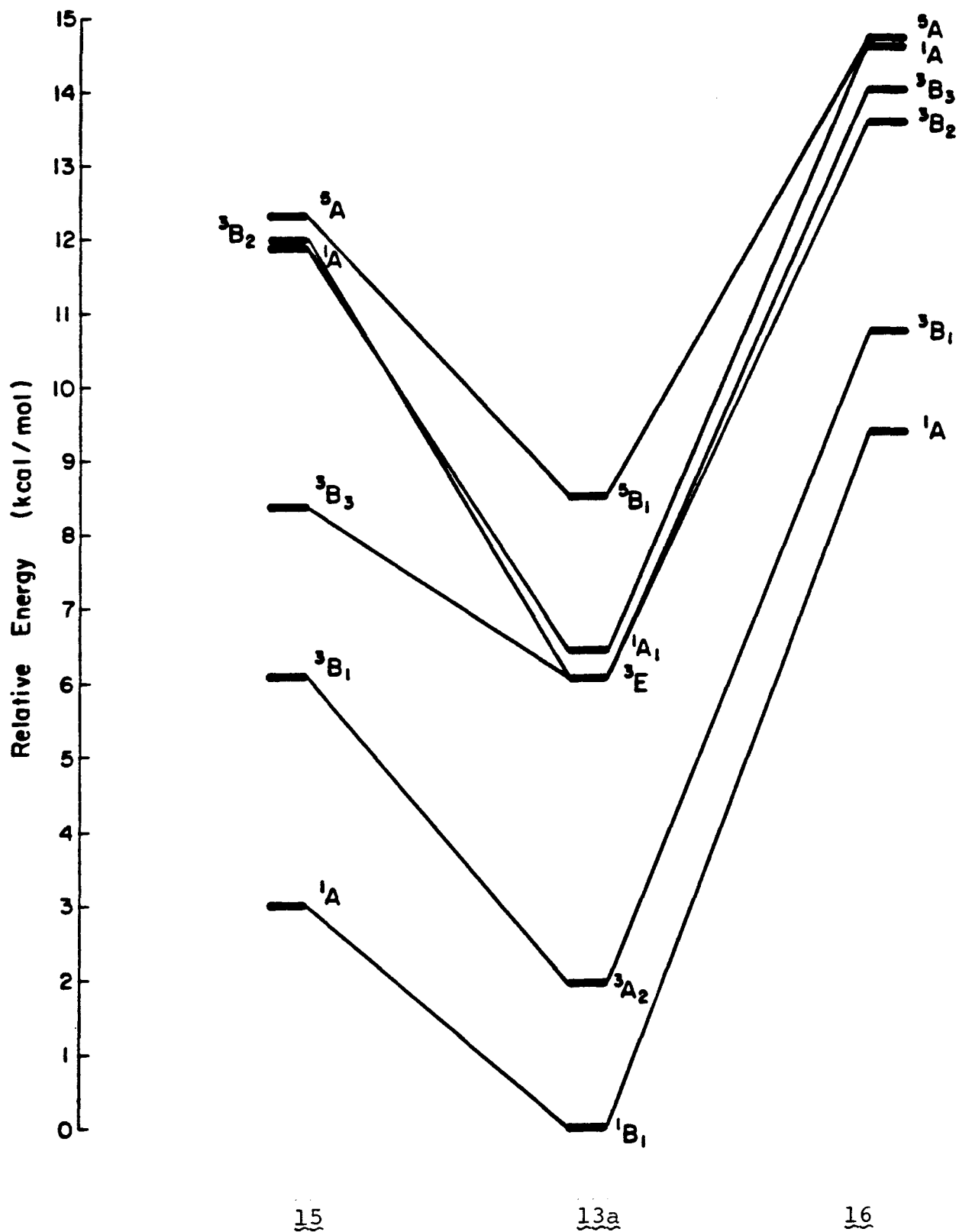
---

<sup>a</sup>Full four electron CI within the a, b<sub>2</sub>, b<sub>3</sub>, b<sub>1</sub> space using the orbitals from the HF solution on the <sup>5</sup>A state. Total energy of the <sup>1</sup>A state: -193.74162 h.

<sup>b</sup>Solution as in a. Total energy of the <sup>1</sup>A state: -193.73152 h.

<sup>c</sup>All energies are relative to the <sup>1</sup>B<sub>1</sub> state of 13a (CI-VDZ).

FIGURE 5. Relative Energies of the Covalent States of 13a and Forms Distorted by the Second Order Jahn-Teller Effect.



The prediction of a significant, although relatively small, stabilization in 7 due to spiroconjugation suggests that 7 lies in a potential energy minimum. Distorting the molecule toward closed shell isomer 10 destabilizes the molecule (Table VII, Figure 5), while ring closure to 9 goes against the "natural orbital correlations". Thus, one might expect potential energy barriers to closure of 7 to 9 or 10, and 7 could thus represent a potential energy minimum. Given that biradical 4 is directly observable at temperatures below 40°K,<sup>23</sup> it seems quite possible that tetraradical 7 will also be observable.

REFERENCES FOR CHAPTER II.

1. Dewar, M. J. S. and Thiel, W. J. Am. Chem. Soc., 1977, 99, 4899-4907, 4907-4917.
2. Chesick, J. P. J. Am. Chem. Soc., 1962, 84, 3250-3253.
3. Conrad, M. P.; Pitzer, R. M.; Schaefer, H. F., III. J. Am. Chem. Soc., 1979, 101, 2245-2246.
4. Salem, L.; Rowland, C. Angew. Chem. Int. Ed. Engl., 1972, 11, 92-111.
5. See, for example, Borden, W. T. "Modern Molecular Orbital Theory for Organic Chemists", Prentice-Hall, Englewood Cliffs, N.J., 1975; pp. 208-212.
6. Borden, W. T.; Davidson, E. R. J. Am. Chem. Soc., 1977, 99, 4587-4594.
7. Borden, W. T.; Davidson, E. R. Acc. Chem. Res., 1981, 14, 69-76, and references therein.
8. Herring, C. in "Magnetism", Rado, G. T. and Suhl, H., Eds., Academic Press, New York, 1966, Vol. IIB, pp. 1-181.
9. Goldberg, A. H.; Dougherty, D. A. J. Am. Chem. Soc., 1983, 105, 284-290.
10. Dunning, T. H., Jr. J. Chem. Phys., 1970, 53, 2823-2833.
11. Huzinaga, S. J. Chem. Phys., 1965, 42, 1293-1302.
12. Bair, R. A.; Goddard, W. A., III., unpublished work.  
Bair, R. A., Ph.D. Thesis, California Institute of Technology, 1982.
13. Bobrowicz, F. W.; Goodgame, M. M.; Bair, R. A.; Walch, S. P.; Goddard, W. A., III, unpublished work.  
Bobrowicz, F. W., Ph.D. Thesis, California Institute of Technology, 1974.



14. Yaffe, L.; Goodgame, M. M.; Bair, R. A.;  
Goddard, W. A., III, unpublished work.
15. Borden, W. T.; Davidson, E. R. J. Am. Chem. Soc., 1980,  
102, 5409-5410. Dixon, D. A.; Dunning, T. H., Jr.;  
Eades, R. A.; Kleier, D. A. Ibid., 1981, 103,  
2878-2880.
16. Bobrowicz, F. W.; Goddard, W. A., III. In "Methods of  
Electronic Structure Theory", Schaefer, H. F., III,  
Ed., Plenum Press: New York, 1977; pp. 77-127.
17. Nobes, R. H.; Bouma, W. J.; Radom, L. Chem. Phys. Lett.,  
1982, 89, 497-500.
18. Davis, J. H.; Goddard, W. A., III. J. Am. Chem. Soc.,  
1977, 99, 4242-4247.
19. Salem, L. and Rowland, C., Angew. Chem. Int. Ed. Engl.,  
1972, 11, 92-111.
20. Walkup, R. E.; Ho, W.; Goddard, W. A., III. Unpublished  
work.
21. Greenberg, A. and Liebman, J. F., "Strained Organic  
Molecules", Academic Press, New York, 1978, pp. 373-374.
22. Würthwein, E.-U.; Chandrasekhar, J.; Jemmis, E. D.;  
Schleyer, P. v. R. Tetrahedron Lett., 1981, 22, 843-846.
23. Buchwalter, S. L. and Closs, G. L. J. Am. Chem. Soc.,  
1979, 101, 4688-4694.

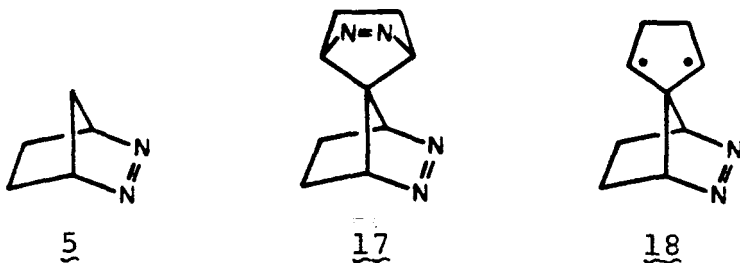
## CHAPTER III.

Experimental Assessment of the Viability  
of 1,4,6,9-Spiro[4.4]nonatetrayl as a  
Reactive Intermediate

The theoretical analysis in Chapter II suggests that 1,4,6,9-spiro[4.4]nonatetrayl 7 should lie in a potential energy minimum. One of the goals of this work has been to determine whether or not 7 is sufficiently stabilized to be a viable reactive intermediate under conventional conditions. Studies were thus undertaken to synthesize potential precursors to 7 and decompose them in solution at ambient temperatures, seeking novel chemistry indicative of the intermediacy of spirononatetrayl.

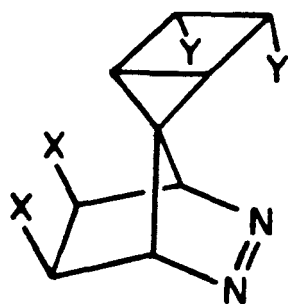
#### A. Potential Precursors to Spirononatetrayl

The thermal and photochemical deazetations of cyclic and polycyclic 1,2-diazenes (azoalkanes) have often been used to generate biradicals.<sup>1,2</sup> Given the successful use of diazene 5 to generate biradical 4<sup>3</sup>, the most obvious precursor to tetraradical 7 was the

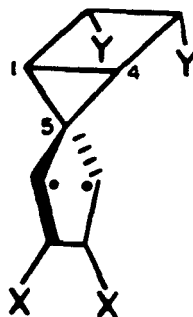


bisdiazene spiro[bis(2,3-diazabicyclo[2.2.1]hept-2-ene)-7,7'], 17. Thermolysis or conventional direct photolysis of 17 could produce singlet biradical 18 either directly or by loss of nitrogen from a diazenyl radical. Ring closure of 18 to give monodiazene 19 should be quite rapid in this case, and would most likely outpace any conceivable competitive

reaction. This path could possibly be circumvented through the use of a very intense light source (such as a laser) which could lead to a two-photon process and direct conversion of 17 to 7. Sensitized photolysis of 17 would produce the triplet state of biradical 18. The lifetime of this species should be much greater than that of the singlet due to the need for intersystem crossing to occur prior to (or concomitant with) ring closure. As such, there is a better chance that triplet 18 could undergo new chemistry. One interesting possibility is a thermal extrusion of the second  $N_2$ , which could occur if the developing spiroconjugative stabilization in 7 significantly stabilized the deazetation transition state.

19

- a**  $X=Y=H$   
**b**  $X=D; Y=H$   
**c**  $X=H; Y=D$

11

Monodiazene 19 is also a potential precursor to 7. Loss of  $N_2$  could produce biradical 11. As discussed in Chapter II, cleavage of the C1-C4 bond in 9 would release ca. 50 kcal/mol of strain energy and allow the full spiroconjugative stabilization of 1 to develop, possibly facilitating the biradical-to-tettraradical conversion. Again, producing the triplet state of 11 through sensitization would

increase the probability of this alternative path being competitive with ring closure.

#### B. Synthesis of Precursor Diazenes

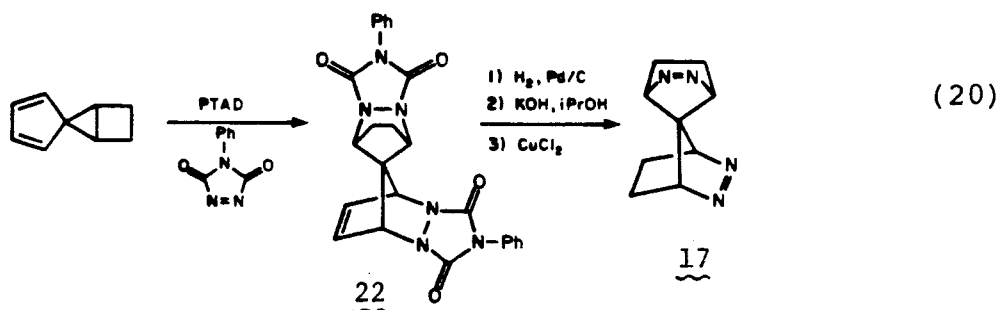
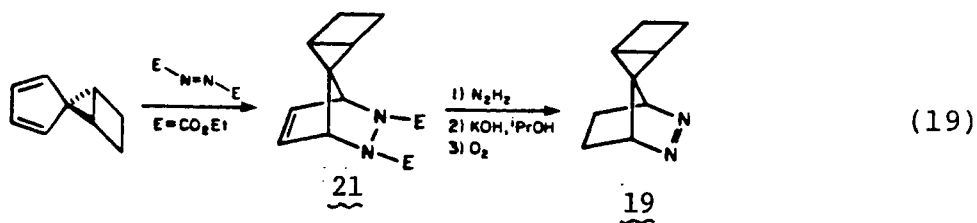
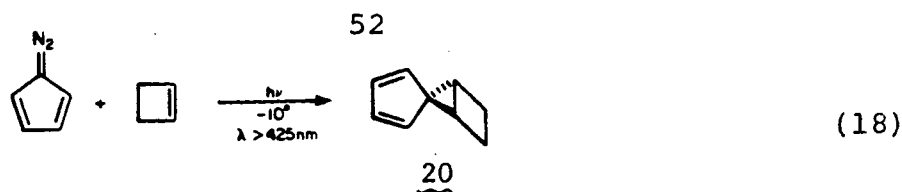
A quite feasible route to bisdiazene 17 would begin with the known<sup>4</sup> 1,3,6,8-spiro[4.4]nonatetraene (8). The standard synthetic sequence<sup>5</sup> by which, for example, cyclopentadiene is converted to 5 should be applicable to 8. In fact, at the time we started this work, the crucial first step of this



8

sequence, the double Diels-Alder addition of dimethyl azodicarboxylate to 8, had been accomplished. However, the synthesis of 8 is lengthy and proceeds in relatively low overall yield.<sup>4</sup> In addition, the tetraene is a relatively reactive molecule.<sup>4,6</sup>

An alternative synthetic approach to 17 and 19 was therefore developed. As shown in eq. 18, photolysis of diazocyclopentadiene in cyclobutene produces spiro[bicyclo[2.1.0]pentane-5,1'-cyclopenta-2',4'-diene], 20. Although the yield of this reaction is low, it does produce in one step a molecule that, for the present purposes, is a complete functional equivalent of tetraene 8. Conversion of diene 20 to monodiazene 19 (eq. 19) follows the usual sequence,<sup>5</sup> with two minor modifications. Catalytic hydrogenation using palladium catalysts is known to cleave cyclopropane rings



faster than olefins are reduced.<sup>7</sup> Diels-Alder adduct 21 was thus hydrogenated with diimide, preserving the bicyclopentane moiety. Due to the well known tendency of strained hydrocarbons to undergo acid-catalyzed rearrangements,<sup>8</sup> the acidic conditions of the standard copper (II) chloride oxidation<sup>5</sup> were also of concern and 19 was produced by air oxidation.

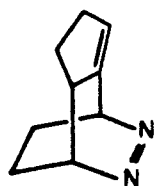
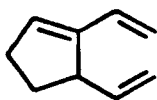
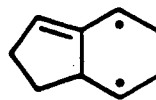
Bisdiazene 17 can also be prepared readily from 20 (eq. 20), the key step being the reaction of 20 with N-phenyltriazolinedione (PTAD). PTAD is a highly reactive dienophile, and it can also add across strained C-C single bonds.<sup>9</sup> In the present case, bisadduct 22 is produced in one step in acceptable yield. Conversion of 22 to 17 follows the standard sequence.<sup>10</sup>

### C. Results and Discussion for Diazene Decompositions.

#### Biradical to Biradical Rearrangements.

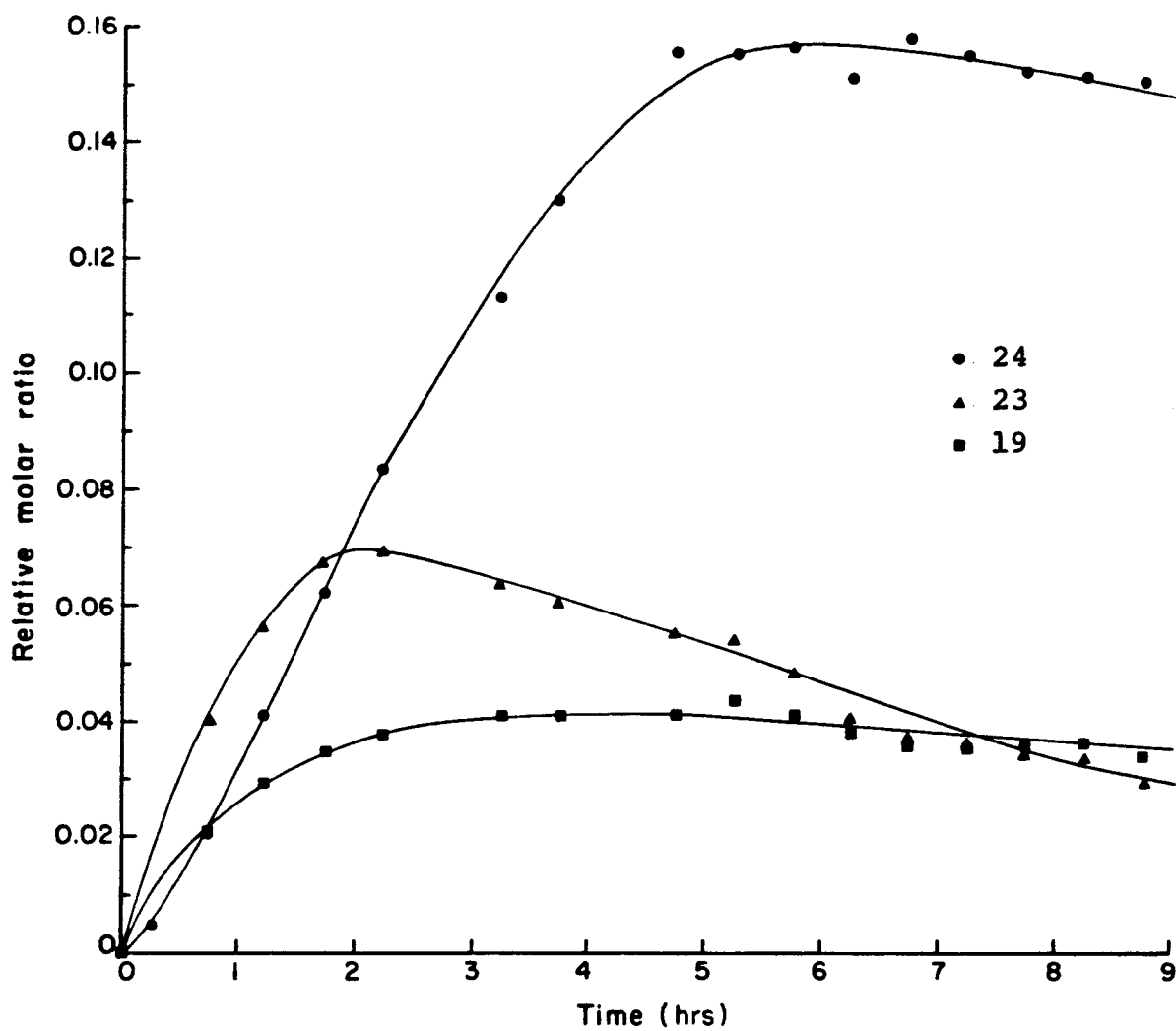
Direct Photolysis of 17. Photolysis of 17 at room temperature using a 450W Hanovia lamp results in N<sub>2</sub> loss and closure to 19 as the sole primary photoproduct. Diazene 19 then undergoes secondary photolysis, as described below.

Sensitized Photolysis of 17. Photolysis of 17 in the presence of benzophenone as a triplet sensitizer results in three major products: biradical closure product 19, the rearranged diazene 8,9-diazatricyclo[5.2.2.0<sup>2,6</sup>]undeca-2,8-diene (23), and the hydrocarbon product 2,3-divinylcyclopentene (24). The changing relative ratios of these products with time are shown in Figure 6.

232425

Diazene 23 arises from a 1,2-alkyl shift in biradical 18 analogous to the trimethylene-to-propene H-shift observed in many other 1,3-biradicals.<sup>11</sup> However, olefin formation is usually observed in singlet 1,3-biradicals (thermolysis or direct photolysis of diazenes) rather than triplets (sensitized photolysis). Ab initio calculations on the singlet and triplet surfaces of trimethylene have led Doubleday and McIver to propose that intersystem crossing from the triplet to the singlet is more favorable at

FIGURE 6. Relative Molar Ratios of Products from the Sensitized Photolysis of 17.





geometries from which closure to cyclopropane proceeds without a barrier once the singlet surface is reached.<sup>11</sup> Thus, triplet biradicals would yield almost entirely cyclopropanes. However, due to the ring constraints, biradical 18 cannot achieve the preferred intersystem crossing geometries and will necessarily come onto the singlet surface in the vicinity of (0,0)-trimethylene. The transition state for the 1,2-H shift to propylene has not been located computationally,<sup>11</sup> but it seems likely that it is near the (0,0) geometry. If so, olefin formation would be more favorable for 18 than for acyclic systems. It is interesting to note that sensitized photolysis of bicyclic diazene 5 which shares the geometrical constraint of 18 does produce ca. 10% of the H-shift product, cyclopentene.<sup>12</sup>

The origin of 24 is less straightforward. One would expect that sensitized photolysis of 23 would produce triplet 1,4-biradical 25, which could then cleave to two olefins, producing 24. Indeed, we have found that 24 is the sole product of sensitized photolysis of 23. As described below, triene 24 is also the major product of sensitized photolysis of 19. Thus, it was possible that 24 arose entirely through sensitized photolysis of the primary photoproducts 19 and 23. However, formation of spiro-nonatetrayl (7) from 17 would also be expected to result in the formation of 24 through the rearrangement pathways described below. Formation of 7 from 17 requires loss of two equivalents of N<sub>2</sub> from a single sensitization event, as the

lifetime of triplet 18 would undoubtedly be too short for a second sensitization to occur. As a test for this possibility, we determined two sensitization quantum yields for 17: one for N<sub>2</sub> evolution (equivalents of N<sub>2</sub> released per sensitization) and one for compound disappearance (equivalents of 17 destroyed per sensitization). Formation of 7 would be evidenced by a greater quantum yield for nitrogen evolution than for diazene disappearance. As can be seen in Table VIII, both quantum yields are equal within experimental error. Therefore, each sensitization causes loss of a single N<sub>2</sub> to give biradical 18, which either undergoes ring closure to 19 or a 1,2-alkyl shift to 23. Initial product ratios indicate that the kinetic ratio of these two processes is greater than 2:1, favoring the alkyl shift. Triene 24 must thus be entirely the product of secondary photolysis. An interesting sidelight of this study is the surprisingly high quantum yield for sensitized photolysis of 23 (Table VIII), compared to the parent system 2,3-diazabicyclo[2.2.2]octene.<sup>13</sup>

Thermolysis and Direct Photolysis of 19. Both thermolysis and direct photolysis of monodiazene 19 lead to a mixture of biradical closure product 9 and 2,3-divinylcyclopentene (24) (Table IX). Control experiments reveal that hydrocarbon 9 does rearrange to triene 24 under the thermolysis conditions, and thus 24 could be entirely a secondary product in this reaction. Direct photolysis also produces

TABLE VIII. Quantum Yields<sup>a</sup> for Sensitized Photolysis of Diazenes

Compound	$^3\phi_{N_2}^b$	$^3\phi_{dis}^c$
<u>17</u>	0.97	0.95
<u>19</u>	0.50	
<u>23</u>		0.65

<sup>a</sup>Values are  $\pm 10\%$ .

<sup>b</sup>For  $N_2$  evolution.

<sup>c</sup>For compound disappearance.

TABLE IX. Product Yields from 19 and 23.

Precursor	Conditions	9	24	Other
19	140°C, 4h	70.6 <sup>a</sup>	29.4 <sup>a</sup>	
19	hν direct	86.7	9.6	3.6
19	hν, Ph <sub>2</sub> CO sensitized	2.3	84.6 <sup>b</sup>	13.0 <sup>b</sup>
23	hν, Ph <sub>2</sub> CO sensitized		100.0	

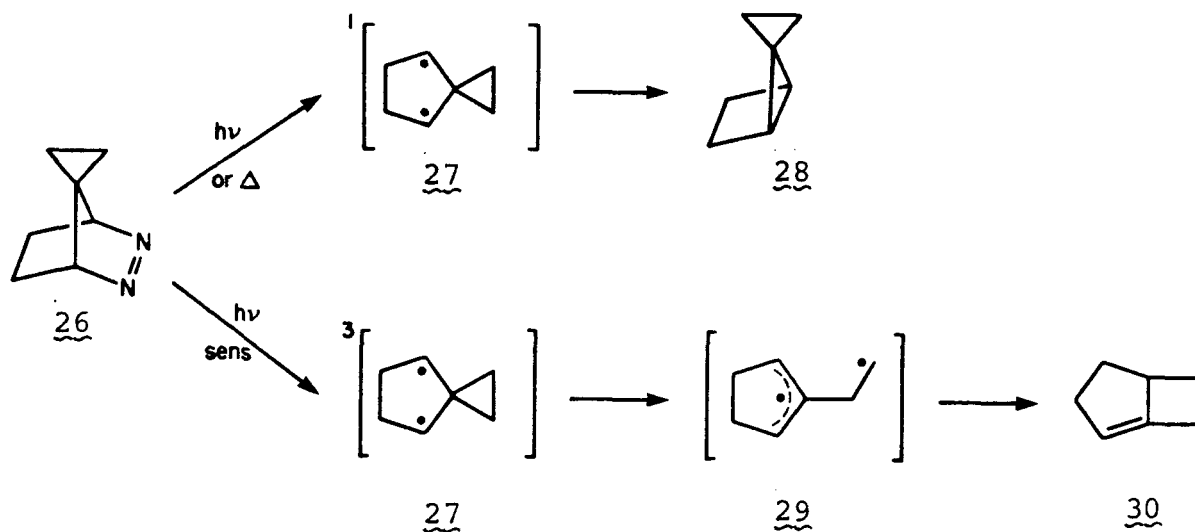
<sup>a</sup>Control experiments indicate that 9 → 24 under these conditions. Values are for 90% conversion of 19.

<sup>b</sup>These products decompose slowly under the reaction conditions. Values are for 90% conversion of 19.

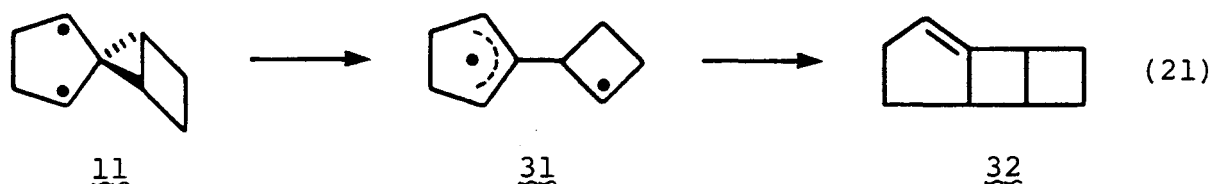
another  $C_9H_{12}$  isomer that we have not been able to identify and that appears to be thermally labile.

Sensitized Photolysis of 19. Benzophenone-sensitized photolysis of 19 yields triene 24 as the major product (Table IX). The overall results for 19 thus parallel Roth's studies on 2,3-diazabicyclo[2.2.1]hept-2-ene-7-spirocyclopropane (26) (Scheme I).<sup>14</sup> Roth found that ring closure was the dominant mode of reaction for single diyl 27, but that the triplet underwent cleavage of the cyclopropane ring to give, ultimately, an olefin product.

Scheme I

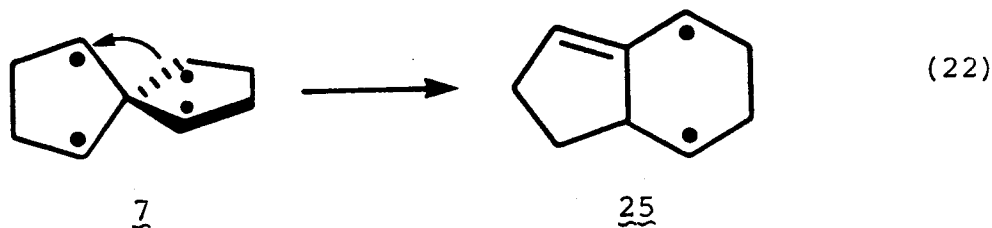


Such a cleavage of a cyclopropane-1,1-dicarbonyl biradical to an "allyl-plus-p" biradical is well-precedented as the second step of the much-studied thermal rearrangement of spiropentanes to methylenecyclobutanes.<sup>15a</sup> By analogy, one would expect triplet 11 to cleave at the C1-C5 bond to give biradical 31 and, ultimately, olefin 32 (eq. 21).



Bicyclo[2.2.0]hexane derivative 32 is highly strained and should be thermally labile. The expected rearrangement of 32 would involve ring opening to biradical 25, and subsequent cleavage of the cyclohexanediyl to produce 24. Starting from the conversion of bicyclo[2.2.0]hexane to 1,5-hexadiene ( $\log A=13.4$ ,  $E_a=36$  kcal/mol)<sup>16</sup> and diminishing  $E_a$  by 11.5 kcal/mol (the difference between cyclobutane and methylenecyclobutane stereomutations)<sup>17</sup> and then by 6 kcal/mol (the approximate difference between the methylenecyclobutane rearrangements of the parent and of bicyclo[3.2.0]hept-1-ene)<sup>14</sup> for inclusion of the five-membered ring, gives an estimate of  $\log A=13.4$ ,  $E_a=18.5$  kcal/mol and  $t_{1/2}(298K) = 1$  sec for conversion of 32 to 24. Thus, formation of 24 can be rationalized in terms of well-precedented reactions.

However, as described above, another rearrangement of biradical 11 seemed feasible, namely C1-C4 cleavage to give spirononatetrayl. One can also envision a rational conversion of tetraradical 7 to triene 24. One surprising feature of the chemistry of spirononatetraene (8) is the ease with which a 1,5-sigmatropic shift of a vinyl group occurs to give, after a hydrogen shift, indene.<sup>6</sup> This result was rationalized by invoking stabilizing, secondary orbital interactions among the formerly spiroconjugating centers. The analogous process in 7 is a 1,2-alkyl shift reaction like that described above for biradical 18. In 7 the migrating center is itself a radical, but the transition state could be stabilized by the same type of secondary orbital interactions as in the rearrangement of 8. The product of such a rearrangement (eq. 22) is biradical 25,



which has already been invoked as a logical precursor to triene 24. In fact, it is already known that triplet 25 produces 24, since 24 is the sole product from sensitized photolysis of 23.

In order to differentiate these two possible pathways to 24, diazene 19b was prepared with completely stereospecific

exo deuterium labeling. Synthesis involved simply substituting  $N_2D_2$  for  $N_2H_2$  in eq. 19. Should the rearrangement to 24 proceed by C1-C5 cleavage only, the cyclopentanediy1 ring of 11b would maintain its integrity throughout the rearrangement (eq. 21) and end up as the cyclopentene ring of 24. Thus, the deuterium label of 19b would appear entirely in the aliphatic  $CH_2$ 's of 24. However, if 7 should intervene, all four  $CH_2$  groups would become equivalent due to the  $D_{2d}$  symmetry of 7. Thus, any 24 derived from the tetraradical would contain an equal mixture of aliphatic (A) and vinylic (V) deuterium label.

Figure 7 shows the  $^2H$  NMR spectrum of 24 produced from the sensitized photolysis of 19b. The spectrum clearly shows the presence of both aliphatic and vinylic label, but in a 4.0:1.0 ratio (Table X).

The excess of 24-A over 24-V from 19b indicates that the C1-C5 cleavage does occur in 11. However, the observation of 24-V requires another mechanism that makes the two five-membered rings of 11 equivalent. Such a process must also produce 24-A, and so a significant portion of the 24-A evidenced in Figure 7 arises from the new mechanism.

If tetraradical 7 is involved in the scrambling mechanism, not only do the two five-membered rings become symmetry equivalent, but both faces of both rings are indistinguishable as well. Thus, there is a second stereochemical test for 7. In diazene 19b, the  $^2H$  labeling has differentiated the two five-membered rings and the two faces of the labeled ring since  $^2H$  incorporation is 100% exo.



FIGURE 7.  $^2\text{H}$  NMR of 24 Derived from the Sensitized  
Photolysis of 19b.

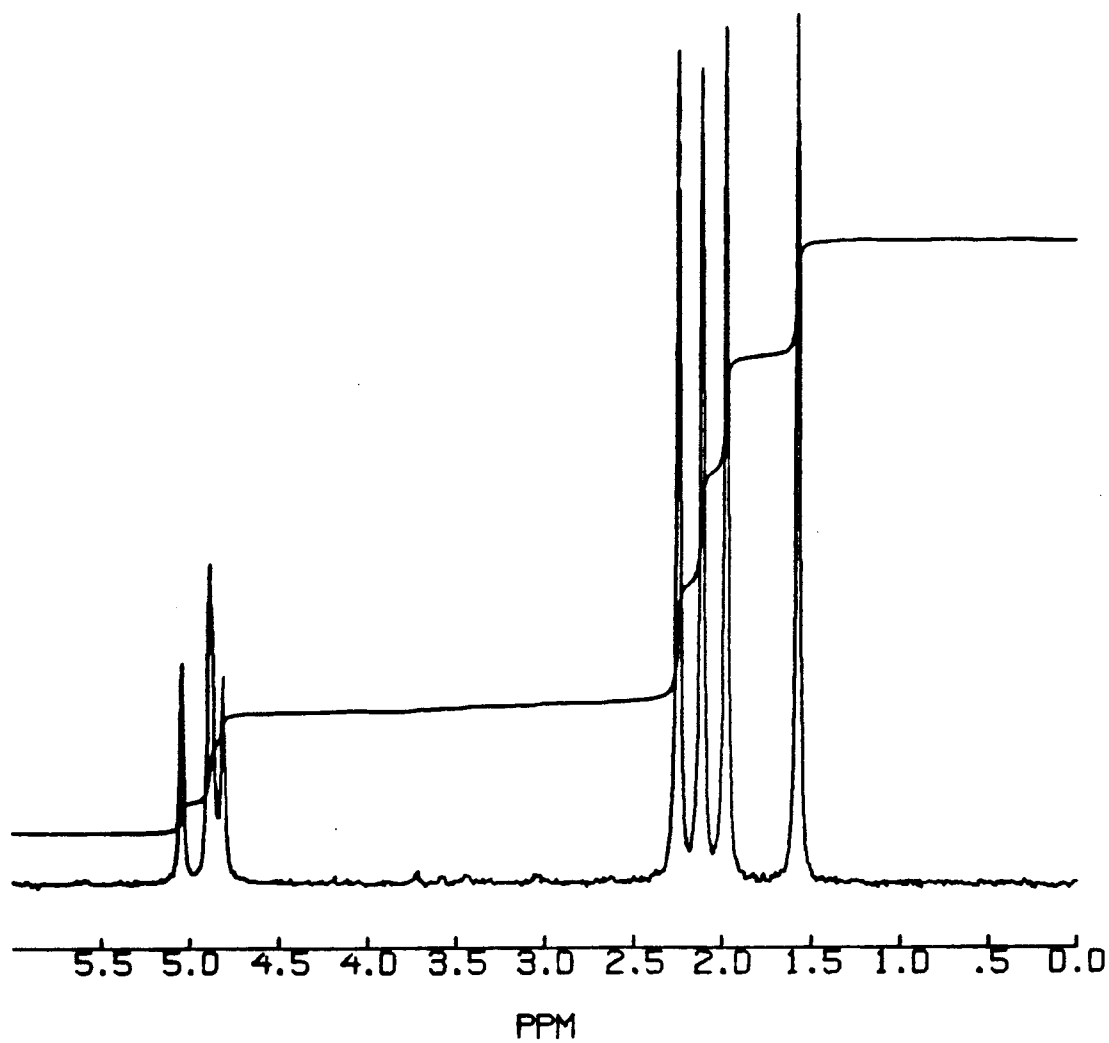


TABLE X. Distribution of  $^2\text{H}$  in 24.

Precursor	<u>24-A:24-V</u> <sup>c</sup>	<u>24-T:24-C</u> <sup>a</sup>
19b	4.0:1.0	1.0:1.0
19c <sup>b</sup>	1.0:3.3	2.3:1.0

<sup>a</sup>Deuterium cis or trans with respect to the proton on C3.

<sup>b</sup>4.0:1.0 endo:exo.

<sup>c</sup>The fact that 24-A/24-V from 19b does not equal 24-V/24-A from 19c suggests a kinetic isotope effect. However, the effects cannot be presently assigned to any particular microscopic event(s).

However, the face-differentiation is lost because the first-formed biradical 11b has a mirror plane of symmetry. Thus, the four aliphatic deuteria in 24 from 19b are in a 1:1:1:1 ratio (Figure 7). Such facial scrambling does not occur in biradical 11c, which would be formed from diazene 19c. As shown in eq. 23, 19c can be prepared from 19b by an "azo transposition" sequence. The key step is the solid state photolysis of 33, using the lattice constraining forces to produce stereospecificity.<sup>18</sup> Using this sequence, 19c is ultimately produced with the <sup>2</sup>H 80% endo and 20% exo (only the endo isomer is shown).

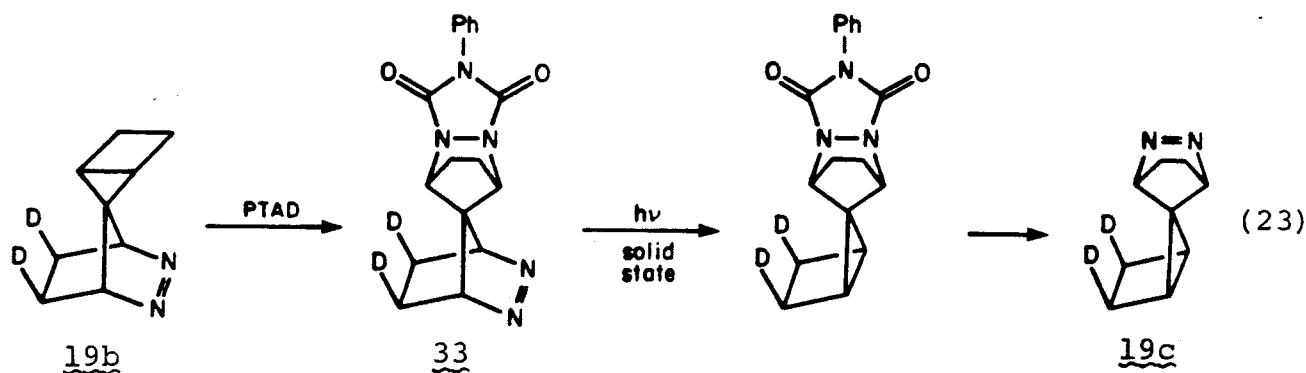
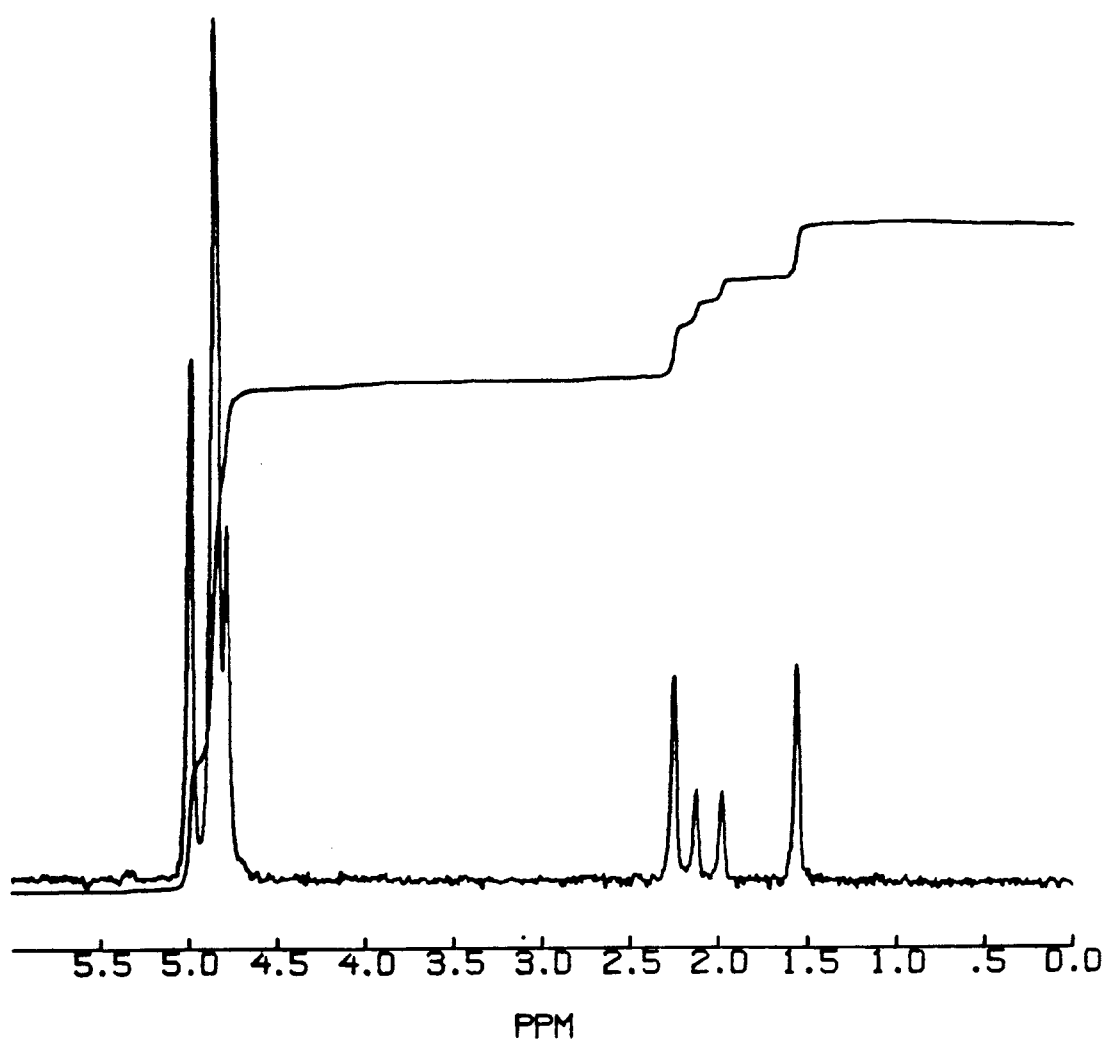
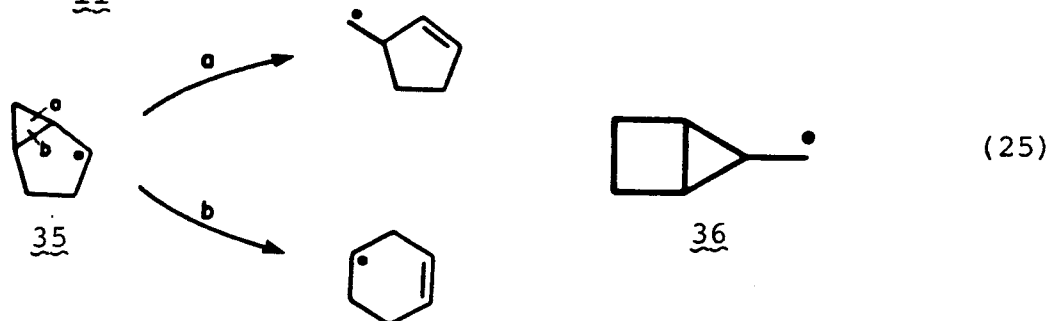
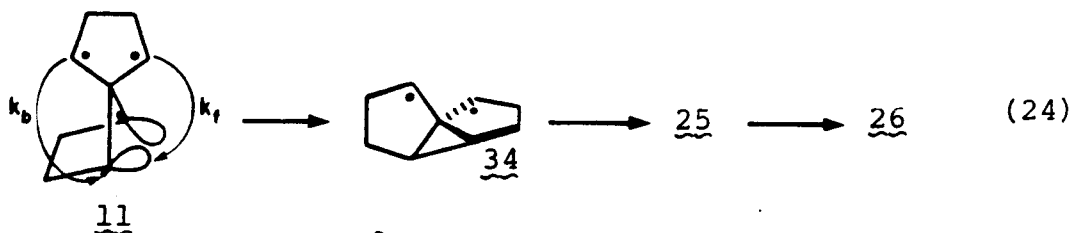


Figure 8 shows the <sup>2</sup>H NMR of 24 obtained from sensitized photolysis of 19c. Again, one sees a mixture of 24-A and 24-V, and in this case the excess of 24-V indicates the presence of the C1-C5 cleavage. However, the preferential formation of 24-T vs. 24-C (Table X) requires a partial scrambling of ring faces. This result requires a new reaction path that interconverts the five-membered rings of 11 but does not lead to complete equivalence of the ring faces. A possible intermediate that would produce such a labeling result is biradical 34, which has only  $C_2$  symmetry.

FIGURE 8.  $^2\text{H}$  NMR of 24 Derived from the Sensitized  
Photolysis of 19c.

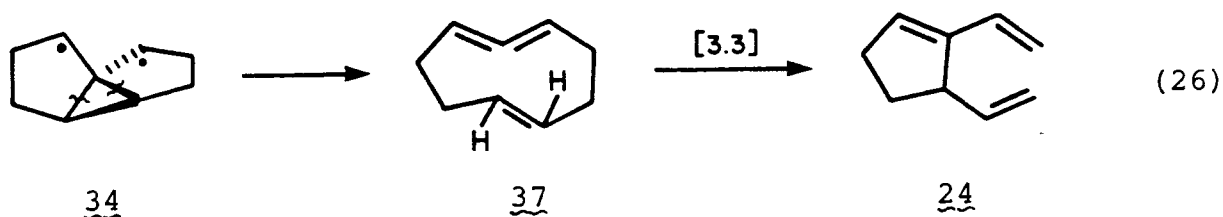


It can arise from 11 by an intramolecular  $S_H$  reaction, with either stereochemical inversion (backside attack,  $k_b$ ), or retention (frontside attack,  $k_f$ ) (eq. 24). The conversion of 34 to 24 has good precedent in free radical rearrangement chemistry. The bicyclo[3.1.0]hex-2-yl radical (35) is known to rearrange readily by paths a and b (eq. 25).<sup>19a</sup> The two paths are equivalent in 34 and give rise to the previously discussed biradical 25. This is also another example of the cyclopropyldicarbonyl to allyl-plus-p rearrangement.



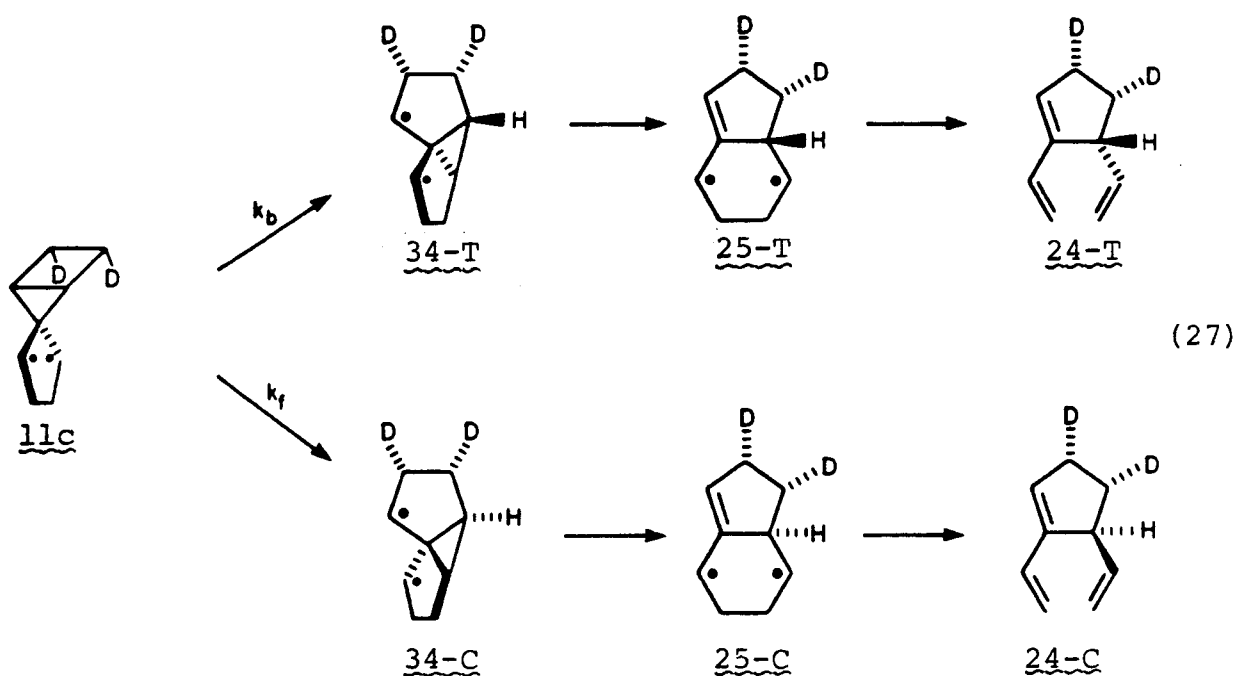
Rearrangement of 35 to the 5-bicyclo[2.1.0]pentylmethyl radical (36) has not been reported.<sup>19a</sup> There is thus no precedent for conversion of 34 back to 11.

It has also been suggested<sup>20</sup> that conversion of 34 to 24 could occur via trans-cyclonona-1,2,6-triene (37). The



allene would be formed by cleavage of two cyclopropyl bonds in 32 (the reverse of addition of a carbene to an olefin) and then undergo Cope rearrangement to 24. Direct observation of 37 has not been reported. Attempts to generate it at low temperature have resulted only in the isolation of 24,<sup>21</sup> suggesting that if formed, 37 could not be observed under the reaction conditions. However, based upon the previously discussed precedents, the allene pathway seems less likely than the biradical-to-biradical rearrangements described above. Intervention of allene 37, should it occur, would in no way alter the results of the deuterium labeling study. Biradical 34 must cleave to the trans olefin and the Cope rearrangement is stereospecific. Thus, the stereochemistry of the deuterium label with respect to the C3 proton in 24 will be set in biradical 34 just as for the biradical-to-biradical rearrangement pathways described above.

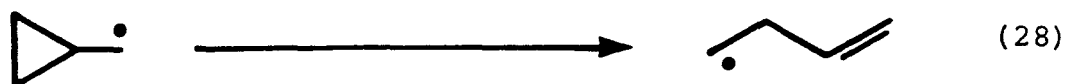
The stereochemical sequences of the intermediacy of biradical 34 are summarized for 24-A from the  $k_f$  and  $k_b$



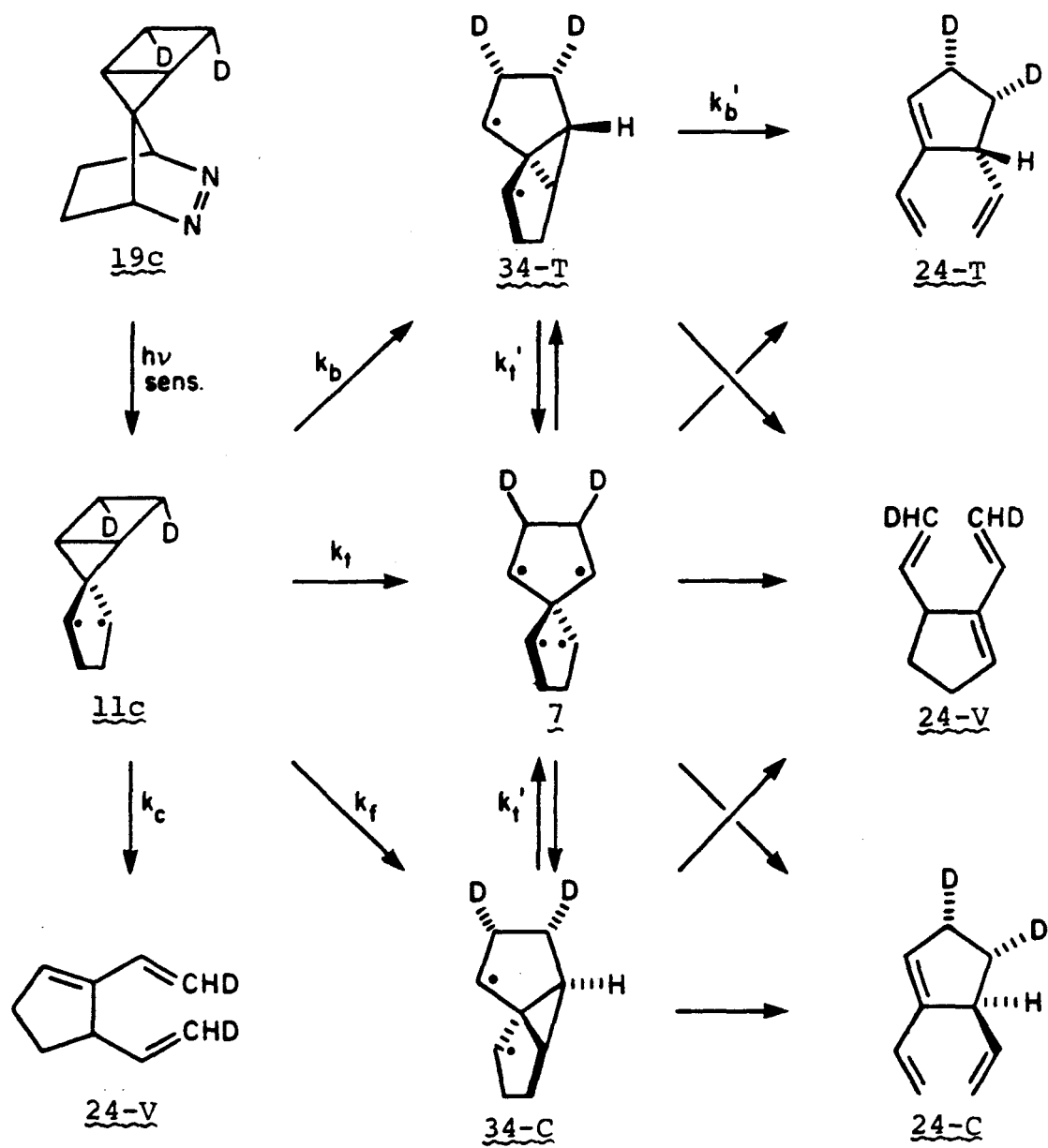
pathways in eq. 27, as well as in the complete overview of our mechanistic model for the system in Scheme II.

There are no data concerning the spin states of the various species in Scheme II. However, it seems certain that 11 is initially formed as a triplet and it seems likely that any biradical in Scheme II that is long-lived enough to undergo rearrangement is also a triplet. The possibility that loss of  $N_2$  from 17 and 19 occurs via diazenyl radicals has been ignored as their intervention would not affect our stereochemical arguments. In addition, there are no experimental data that indicate the intervention of a diazenyl radical in the sensitized photolysis of a pyrazoline.

The scrambling of the  $^2H$  label between the two five-membered rings is incomplete starting from either 19b or 19c, as shown by the 24-A:24-V ratios. We interpret this to mean that the C1-C5 cleavage mechanism ( $k_c$ ) must be operative. This is the biradical version of a cyclopropylcarbinyl-to-allylcarbinyl ring opening.<sup>19b</sup> In the parent radical (eq. 28), such a process is quite facile. One might expect that in the biradical case the reaction would be



further accelerated by the developing allylic stabilization of the other radical site. As discussed above, the  $k_c$  process

Scheme II



is also well known in biradical chemistry, being the second step of the spiropentane rearrangement.<sup>15a</sup> Nevertheless, our labeling results require other processes to be competitive. Perhaps, the  $k_c$  reaction in the present system is retarded by stereoelectronic factors, since the radical p orbitals in the preferred conformation are not directly aligned with the cleaving bond.<sup>19b,22</sup> Further work is under way to investigate this possibility.

The ring scrambling pathways can best be discussed in terms of the 24-C to 24-T ratio from 19c. Within the framework of the current model (Scheme II), the preferential formation of 24-T from 19c requires the operation of the backside attack ( $k_b$ ) mechanism. Although one could envision a scheme to produce 24-A from 19c involving only the  $k_c$  path, by first interconverting 11c and 11b via 34, such a path must produce a 1:1 ratio of 24-C to 24-T, as the facial distinction is lost in 11b. Also, as discussed above, there is no free radical precedent for 34  $\rightarrow$  11. The stereochemical alignment for this backside attack ( $k_b$ ) is far removed from the 180° angle which is strongly preferred in related reactions.<sup>23</sup> However, the unusual steric constraints of this system and the high strain of the C1-C4 bond in 11 must conspire to make this process competitive with  $k_c$ .

In order to rationalize the formation of 24-C from 19c, either frontside attack in 11 ( $k_f$ ) or tetraradical formation ( $k_t$  or  $k_t'$ ) must be invoked. Frontside free radical attack on a C-C bond (stereochemical retention) is

unprecedented, and a variety of studies has found a strong preference for backside attack.<sup>23</sup> Again, however, the unusual stereoelectronic features of our system and the high strain of the C1-C4 bond could facilitate the  $k_f$  process.

Alternatively, the formation of 24-C could signal the intervention of tetraradical 7. One can envision two pathways to 7 (Scheme II), and once formed, the tetraradical must produce 24-V, 24-C and 24-T in a 2:1:1 ratio. The first route to 7 assumes that only the  $k_b$  process is competitive with  $k_c$ . Once formed, biradical 34-T undergoes both cleavage to biradical 25 (eq. 24), leading to 24-T, and interconversion with 34-C via tetraradical 7 ( $k_t'$ ). Due to its high symmetry, 7 cannot be a transition state for the interconversion of 34-T and 34-C, and thus seems likely to be a reactive intermediate.<sup>24</sup>

The other route to 7 involves the previously discussed direct conversion of 11 to 7 ( $k_t$ ), in competition with both  $k_b$  and  $k_c$ . Ring opening of the bicyclopentane moiety in 11 must be disrotatory, and the back lobes of the C1-C4  $\sigma$  bonding orbital would come into a much more favorable position for bonding with the cyclopentanedyl radical centers as the bond is cleaved. Thus, one would have a competition between complete scission of the C1-C4 bond ( $k_t$ ) and intramolecular backside trapping of the incipient cyclopentanedyl ( $k_b$ ). Table XI shows the relative rates that would be necessary to reconcile each mechanistic scenario with the observed product ratios.

TABLE XI. Relative Rates for Biradical-to-Biradical Rearrangements Leading to 24.

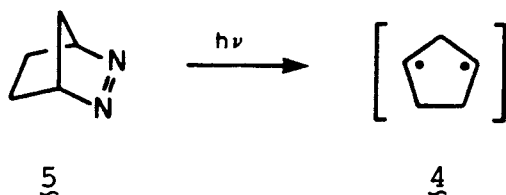
Source of <u>24-C</u> from <u>19c</u>	Relative Rate			
	<u>k<sub>c</sub></u>	<u>k<sub>b</sub></u>	<u>k<sub>f</sub></u>	<u>k<sub>t</sub></u>
<u>k<sub>f</sub></u>	1.0	0.72	0.15	
<u>k<sub>t</sub></u>	1.0	0.57		0.30
<u>k<sub>t</sub></u> <sup>a</sup>	1.0	0.89		

<sup>a</sup>For this mechanism  $k_b'/k_t'$  must be 0.57/0.30.

Once formed, 7 could lead to products through a single ring closure to 34 followed by cleavage to first 25 and then 24, or through the previously discussed 1,2 alkyl shift to 25 (eq. 22), or by a return to 11 followed by  $k_b$  and  $k_c$  pathways. Our labeling studies only indicate that some symmetrization has occurred, and thus do not allow distinctions among these pathways to be made.

#### D. Electron Spin Resonance Studies on Diazene Decompositions

This work is in part derived from the successful observation of cyclopentanediy1 by Buchwalter and Closs.<sup>3</sup>

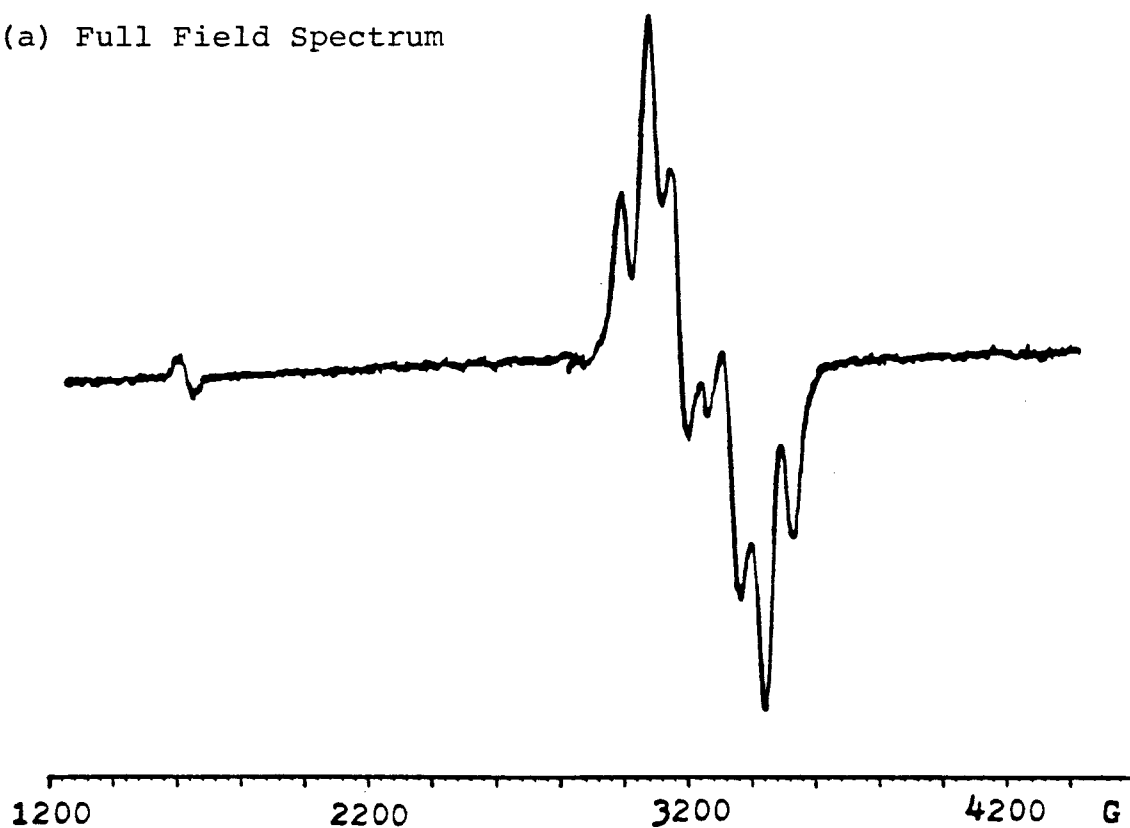


Their generation of the ESR signal of a triplet biradical suggested photolysis of the previously discussed diazenes at low temperatures in the cavity of an ESR spectrometer as a means of observing tetraradical 7.

Irradiation of a 2-methyltetrahydrofuran (MTHF) matrix containing 19 at 8 K led to the ESR spectrum pictured in Figure 9. The presence of a half-field,  $\Delta m_s = 2$  peak identifies the carrier of the signal as a triplet species and the position of the  $\Delta m_s = 1$  signal allows calculation of the zero-field splittings as  $|D/hc| = 0.0255 \text{ cm}^{-1}$  and  $|E/hc| = 0.0030 \text{ cm}^{-1}$ . A Curie plot<sup>25</sup> of signal intensity vs. inverse

FIGURE 9. ESR Spectrum Obtained upon Irradiation of a MTHF Matrix Containing 19 at 8 K.

(a) Full Field Spectrum



(b) Hyperfine Structure on the  $\Delta m_s = 2$  Peak



temperature was linear indicating a triplet ground state for the biradical (Figure 10).<sup>26</sup> An identical signal was observed from direct photolysis of bisdiazene 17 under the same conditions (Table XII). This result is not surprising as the primary photoproduct of 17 under direct photolysis is 19. The difference in rise time of the signal from the two precursors (ca. 3 min for 19, ca. 45 min for 17) suggests that for both diazenes, the immediate precursor to the signal is 19.

The identity of the biradical derived from 19 is uncertain. However, there are logical candidates that can be eliminated. One of these, unfortunately, is spiro-nonatetrayl. In the  $D_{2d}$  symmetry of 7, the symmetry



7

equivalence of the x and y axes dictates a zero field splitting  $|E/hc| = 0$ . That is, the ESR spectrum of 7 should contain only four components of the  $\Delta m_s = 1$  peak, not six as does the spectrum in Figure 9. It is, of course, possible that 7 would not possess  $D_{2d}$  symmetry but ab initio calculations indicate the molecule is stable to symmetry lowering by second order Jahn-Teller distortion (see Chapter II). In addition, ab initio calculations also predict a singlet

FIGURE 10. Curie Plot for the Triplet Species Generated upon Photolysis of 19.26

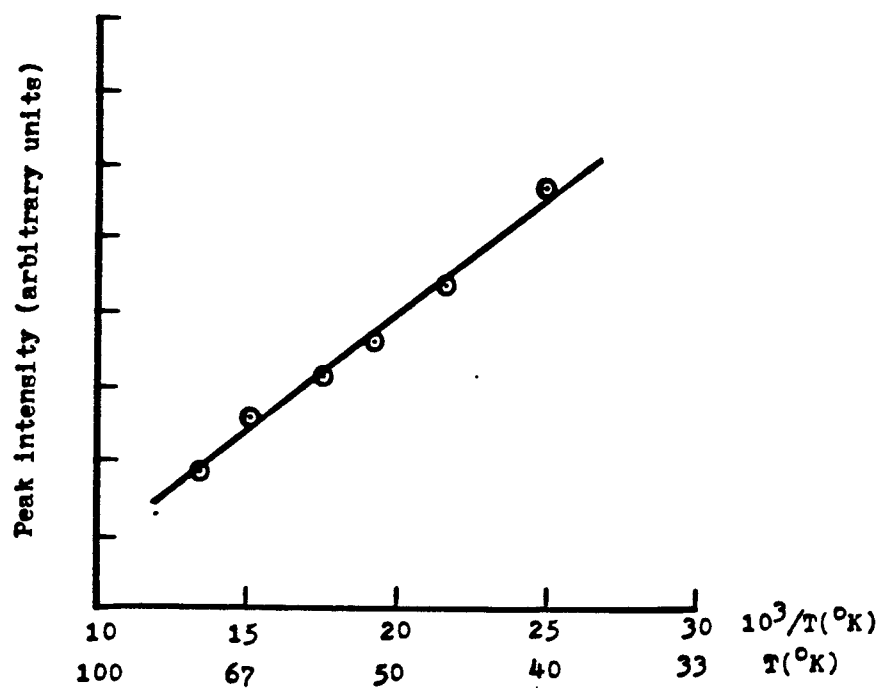
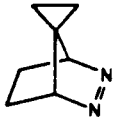
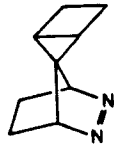
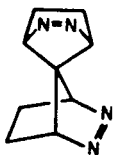
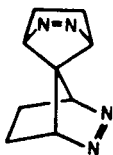
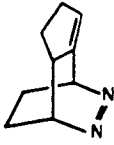
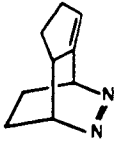


TABLE XII. Zero Field Splitting Parameters for Biradicals Derived from Various Diazenes.

Precursor	[Precursor] ( <u>M</u> )	[Ph <sub>2</sub> CO] ( <u>M</u> )	$ D/hc $ (cm <sup>-1</sup> )	$ E/hc $ (cm <sup>-1</sup> )
 <u>26</u>	0.100		0.0264 <sup>27,a</sup>	0.0035 <sup>27,a</sup>
 <u>19</u>	0.100		0.0255	0.0030
 <u>17</u>	0.029		0.0253	0.0031
 <u>17</u>	0.029	0.250	0.0260	0.0043
 <u>23</u>	0.014		No Signal	
 <u>23</u>	0.027	0.333	0.0256	0.0045

<sup>a</sup>Repetition of the experiment in this work gave the same values.




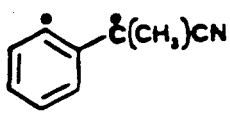
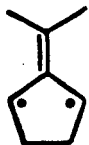
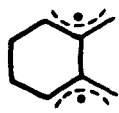
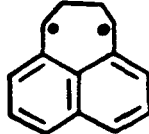


ground state for 7 while the Curie plot shown in Figure 10 implies a triplet ground state for the carrier of the signal.

Another possibility that can be discounted is biradical 11. Table XIII lists zero field splitting param-



eters for a number of triplet biradicals. One would expect 11 to give a signal similar to 1,3-cyclopentanediy1 ( $|D/hc| = 0.084 \text{ cm}^{-1}$ ,  $|E/hc| = 0.002 \text{ cm}^{-1}$ ), but the observed splitting instead falls within the range found for delocalized biradicals and is in fact remarkably similar to the values for the two trimethylenemethanes (TMM) listed in Table XIII.  $|D/hc|$  values for the two localized biradicals are larger by more than a factor of three, suggesting that the biradical derived from 19 is in fact delocalized. Although it is conceivable that the two radical centers could delocalize onto the cyclopropane ring of 11, ab initio calculations of the zero field splitting for 27<sup>26</sup> indicate only a minor decrease relative to 4. In addition, the bridge flip barrier in 28 is only 10 kcal/mol smaller than that in bicyclo[2.1.0]pentane (6) - a difference that is easily explained in terms of the release of spiro strain in 28 that is not present in 6.<sup>14</sup> It thus seems that there is insufficient interaction between the radical

TABLE XIII. Zero Field Splitting Parameters for Various Biradicals.<sup>3</sup>

Biradical	$ D/hc $ ( $\text{cm}^{-1}$ )	$ E/hc $ ( $\text{cm}^{-1}$ )
	0.024	0
	0.1069	0.0058
 <u>1</u>	0.027	0.0023
	0.0204	0.0016
	0.018	0.003
 <u>4</u>	0.084	0.0020
	$0.112^{28}$	$0.0050^{28}$

electrons and the cyclopropane ring in 11 to decrease the zero field splitting to the observed value.

Another factor that argues against 11 as the carrier of the ESR signal from 19 is the thermal stability of the species. The biradical is stable until the softening of the matrix at ca. 85 K. In contrast, biradical 4 has only a 15 minute half-life at 8 K.<sup>3</sup> Admittedly, at low temperatures, the decay of 4 occurs primarily via tunneling of the methylene group<sup>3</sup> and such a process would be expected to be less favorable in 11, where the mass of the tunneling group would be much greater. However, at temperatures higher than 20 K, decay of 4 occurs via classical passage over a 2.3 kcal/mol barrier. For 11 to be indefinitely stable at 85 K,  $E_a$  for closure must be at least 5 kcal/mol (assuming  $\log A=8$ , as for decay of 4<sup>3</sup>) and probably higher. It is difficult to see a structural feature of 11 that would raise the ring closure barrier relative to 4 to that extent, suggesting that 11 is not the carrier of the signal.

Similar arguments beset biradical 34, the product of free radical attack on the bicyclopentane bond of 11. As a

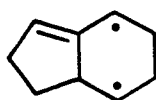
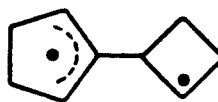


34

localized biradical, the D-value of 34 would be expected to be much higher than that observed. Calculations based on the point charge method predict  $|D/hc|$  to be  $0.108 \text{ cm}^{-1}$ .<sup>26</sup>

Again, electronic interaction with the cyclopropane ring is a possibility, but alignment of the radical p orbitals with the cyclopropane Walsh orbital is poor. In addition, the radical orbitals are contained in a (60,60)-trimethylene unit, for which a singlet ground state is predicted by ab initio calculations.<sup>29</sup>

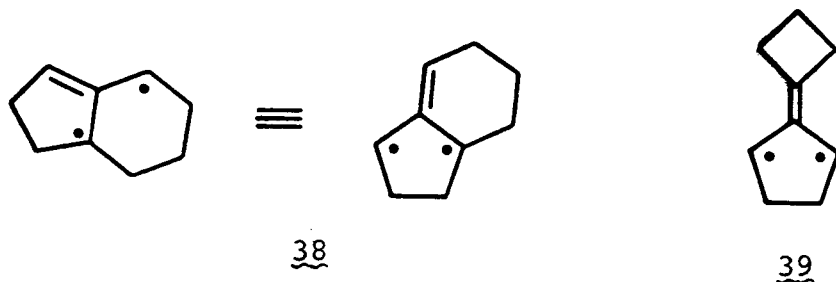
Other possibilities included the "allyl-plus-p" biradicals 25 and 31, that have previously been invoked in

2531

the rearrangements following sensitized photolysis of 17 and 19 at ambient temperature. Zero field splittings for such species had not been reported but delocalization of one radical electron in the allyl group could result in the lowered  $|D/hc|$  value observed. It was also possible that allyl resonance would raise the activation energy for ring closure and provide the stabilization necessary for persistence at 85 K. It could be argued that formation of either 25 or 31 requires a rather deep seated rearrangement for 8 K, but after elimination of the first formed biradical 11 from consideration, one is left with the conclusion that either the rearrangement pathways have low activation energies (formation of 25 or 31 from 11 will be exothermic) or

there is a tunneling process leading to the carrier of the signal.

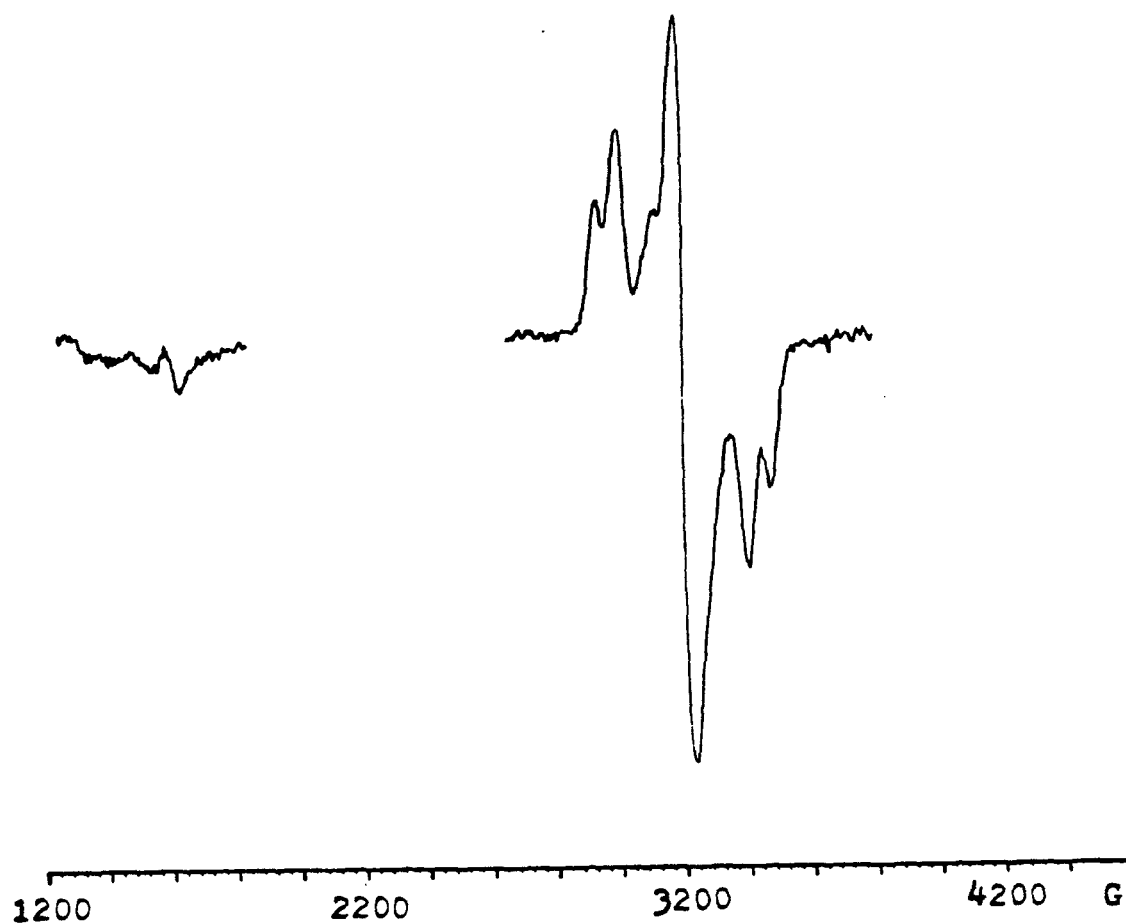
Consideration of the "allyl plus p" biradicals suggests two more possibilities, TMM derivatives 38 and 39, produced



by a 1,2-H shift in 25 and 31, respectively. Hydrogen shifts are known<sup>30</sup> to occur by tunneling at low temperatures, making 38 and 39 equally as viable as 25 and 31. In addition, the ESR signal from 19 possesses zero field splittings consistent with the TMM moiety (Table XIII).

Entry into the bicyclo[4.3.0]nonane ring system (biradicals 25 and/or 38) is provided by photolysis of diazene 23. Presumably the first formed hydrocarbon biradical would be 25 which then might be followed by 1,2-H shift to 38. Direct photolysis of a MTHF matrix containing 23 did not give rise to an ESR signal. This result was not unexpected as photolysis of the parent compound 2,3-diazabicyclo[2.2.2]octene also does not produce a signal.<sup>3</sup> Addition of benzo-phenone to the MTHF matrix before photolysis leads to the spectrum pictured in Figure 11, with zero field splittings listed in Table XII. In a propylene glycol matrix, the

FIGURE 11. ESR Spectrum Obtained upon Irradiation of a MTHF Matrix Containing 23 at 8 K.



signal is still observable above 100 K. This spectrum is also observed during sensitized photolysis of bisdiazene 17 under the same conditions. Since sensitized photolysis of 17 leads primarily to 23 (see Figure 6), it seems logical that the observed signal derives from secondary sensitization.

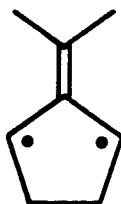
As can be seen by comparison of Figures 10 and 11, the species produced by decomposition of 23 is not that derived from 19. Although the D-values for the two spectra are equal within experimental error, the E-values are significantly different. In addition, the biradical from 23 is accompanied by a large doublet signal, suggesting its mode of reactivity is different from the species from 19, whose spectrum is not superimposed upon a doublet.

This leaves among the viable candidates 31 and 39. It is worth noting that photolysis of diazene 26 leads to a triplet biradical with zero field splitting parameters<sup>27</sup> and thermal stability similar to those from the photolysis of 19,

2940

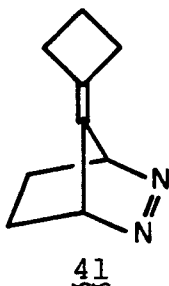
suggesting structural similarity as well. The analogous candidates for this biradical are 29 and 40. The biradical from 26 is stable even to 146 K in a propylene glycol matrix.<sup>26</sup> Extrapolating this result to the biradical from 19 (perhaps not justifiably), one is left with a hypothetical pair of "allyl plus p" biradicals (29 and 31) that do not undergo ring closure at 146 K. Given that there do not seem to be steric or orbital alignment barriers to closure and that the matrix sites must be sufficiently flexible to allow rearrangements of the carbon skeletons in order for ESR signals to be observed, it appears that 29 and 31 are unlikely to be the species in question.

The TMM derivatives (39 and 40) seem much more viable candidates as they share the 2-alkylidene-1,3-cyclopentane-diyl moiety that has been exploited so elegantly by Berson.<sup>31</sup> Triplet biradical 1 can be observed by ESR at temperatures

1



as high as 268 K,<sup>31</sup> correlating well with the observed thermal stability of the biradicals from 19 and 26. In addition, a Curie plot of 1 indicates a triplet ground state for the biradical and the zero field splitting parameters for 1 are very similar to those for species derived from 19 and 26. One of the current projects in this laboratory is the synthesis of diazene 41 as a means to generate 39 independently.



A discussion of these results cannot be considered complete without the standard caveats on the pitfalls of ESR studies. Lengthy consideration of biradical 39, for which there is no evidence in the previously described room temperature solution phase studies, illustrates the first. Due to the extreme sensitivity of the method, the observed species can be representative of a very minor pathway in the reaction. Low temperature work adds a further complication by possibly suppressing the ambient temperature chemistry and allowing tunneling processes to become dominant. In view of these considerations, it should be emphasized that the candidates discussed in this section by no means represent an exhaustive list of the possibilities. It should also be mentioned that observed species can be derived from an impurity in the starting material. However,

given that similar signals arise from diazenes 17, 19, and 26, for which the synthetic details differ, it seems unlikely that similar impurities would be found in each. Another problem with ESR studies is that triplet radical pairs arising through hydrogen abstraction from the matrix can give spectra that mimic triplet biradicals. However, that is most unlikely to be the case here as 19 gives rise to the same ESR signal (superimposed with varying amounts of doublet) in microcrystalline powder and matrices of MTHF, hexafluorobenzene, and mixtures of 2- and 3-methylpentane.

In conclusion, photolyses of diazenes 17, 19, and 26 all give rise to triplet biradicals whose ground state spin multiplicity, zero field splitting parameters, and thermal stability are consistent with the TMM moiety. Although positive identifications of the species are not possible at this time, they are probably delocalized biradicals and structures containing the bicyclo[4.3.0]nonane ring system are unlikely due to the results from photolysis of diazene 23.

## E. Conclusions

The present work describes our initial efforts at determining the viability of an organic tetraradical as a reactive intermediate. The chemistry of bisdiazene 17 gives no indication that 7 is involved under conventional conditions. Sensitized photolysis of 17 does lead to the novel rearrangement product 23. Still to be probed is the potential for two-photon photochemistry in 17. Similarly, thermolysis and direct photolysis of diazene 19 are relatively straightforward.

In contrast, the stereochemical labeling studies of the sensitized photolysis of 19 unambiguously indicate the operation of new biradical-to-biradical rearrangement pathways. Biradical-to-biradical rearrangements are relatively uncommon and could provide a wealth of valuable information on these reactive species. This work and the work of others<sup>32</sup> demonstrate the value of preparing triplet biradicals, for which ring closure is spin-forbidden, in studies of biradical rearrangements. Our current mechanistic scheme (Scheme II) requires at least three biradical rearrangement pathways. The first is the preceded cleavage of biradical 11,  $k_c$ , a process consistent with the accepted mechanism of the spiropentane rearrangement.<sup>15a</sup> In addition, we propose the novel, backside, intramolecular  $S_H$  reaction,  $k_p$ , which is unique in its substantial deviation from the usual alignment for radical additions. The third process involves completely unprecedented chemistry, either

in the form of a frontside radical attack on a C-C bond ( $k_f$ ), or in the formation of tetraradical 7. Thus, the suspicion that new and interesting chemistry would occur on the  $C_9H_{12}$  potential energy surface<sup>15b</sup> in the vicinity of tetraradical 7 was confirmed, although thus far, only permissive rather than compelling evidence for the direct involvement of 7 has been found. Work is in progress to further characterize the novel biradical rearrangements uncovered in the present work, and to investigate the viability of 17 and 19 as precursors to 7 under cryogenic, matrix-isolation conditions.

## F. Experimental Section

General. Pentane was extracted with  $\text{H}_2\text{SO}_4$ , passed through a column of alumina and distilled. Benzene was refluxed over  $\text{P}_2\text{O}_5$  and stored over 4 A molecular sieves. Reagent grade acetone, 95% ethanol, absolute ethanol, and HPLC grade ethyl acetate were used as purchased.

Photolyses were performed with a Hanovia 450 W medium pressure mercury arc lamp.

$^1\text{H}$  NMR spectra were recorded on a Varian EM-390 spectrometer. Fourier transform NMR spectra ( $^1\text{H}$  and  $^{13}\text{C}$ ) were recorded on a JEOL FX-90Q or a Varian XL-200 spectrometer.  $^2\text{H}$  NMR (77.8 MHz) and 500 MHz  $^1\text{H}$  NMR spectra were recorded on a Bruker WM500 spectrometer. Ultraviolet spectra were recorded on a Beckman Model 25 spectrophotometer. Mass spectra were obtained by the Caltech Analytical Facility. Elemental analysis was performed by Spang Microanalytical Laboratory, Eagle Harbor, Michigan or by the Caltech Analytical Facility. Analytical gas chromatography was performed on a Hewlett-Packard 5840A or 5880A chromatograph equipped with a flame ionization detector. Preparative gas chromatography was performed on a Varian Aerograph Model 920 chromatograph with a thermal conductivity detector. Columns for Gas Chromatography:

Column A: 5' x 1/4" 15% OV-101 on Chrom G mesh size 100/120.

Column B: 10' x 1/4" 10% UCW-982 on Chrom WAW-DMCS mesh size 80/100.

Column C: 8' x 1/4" 15% SE-30 on Chrom WAW-DMCS mesh size 80/100.

Column D: 20" x 1/8" 10% UCW-982 on Chrom WAW-DMCS mesh size 80/100.

Column E: 30 m x 0.032 mm DB-1 25  $\mu$  film on fused silica.

Column F: 30 m x 0.032 mm DB-5 25  $\mu$  film on fused silica.

Cyclobutene. Cyclobutene was made by the method of Cope.<sup>33</sup>

Tosyl Azide. 71.5 g (1.10 mole) of sodium azide was dissolved in 300 ml of 95% ethanol. To this solution was added 190.5 g (1.00 mole) *p*-toluenesulfonyl chloride in 800 ml reagent grade acetone. A precipitate of NaCl formed immediately and the supernatant liquid turned orange. The reaction mixture was stirred for 15 hours, then filtered. Acetone was removed by rotary evaporation and the organic phase separated and diluted with 100 ml CH<sub>2</sub>Cl<sub>2</sub>. The solution was washed three times with distilled water and dried over Na<sub>2</sub>SO<sub>4</sub>. Removal of the solvent left 185.0 g of tosyl azide (92% yield, 98.6% pure by NMR analysis).

Diazocyclopentadiene. Diazocyclopentadiene was made by a modification of the method of Weil and Cais.<sup>34</sup> 50.1 g (0.250 mole) of tosyl azide was placed in a flask cooled to 0°C. Ethanolamine (13.5 ml, 0.223 mole) was added and stirring begun. Cyclopentadiene (20.0 ml, 0.243 mole) was then

added and the mixture left to stir at 0° for 4.5 hours. The brick-red slurry was washed with pentane until the washings were light yellow and the pentane solution extracted with distilled water until the aqueous phase was neutral by pH paper. Pentane was removed and the crude diazocyclopentadiene stored in the freezer. Samples were trap-to-trap distilled at room temperature and 0.5 torr and collected at -78°C immediately before use.<sup>35</sup>

Spiro[bicyclo[2.1.0]pentane]-5,1'-cyclopenta-2',4'-dienel (20). Cyclobutene (11.5 g, 0.213 mole) was vacuum transferred into a tube equipped with a stopcock and a side arm closed with a serum cap. Diazocyclopentadiene (0.750 ml, 8.62 mmole) was added by syringe. The solution was irradiated for 6 hours at -20°C through a Corning 3-73 filter (cutoff 415 nm). The remaining cyclobutene was recovered by vacuum transfer and the procedure repeated until all cyclobutene was consumed. The combined photolysis products were purified by flash chromatography<sup>37</sup> on silica gel (EM Silica Gel 60, 230-400 mesh), eluting with petroleum ether. Total yield was 778 mg of spirodiene 20. Analytical samples were purified by preparative gas chromatography on column A (oven temperature 75°, gas flow 23 cm<sup>3</sup> He/min). <sup>1</sup>H NMR (CDCl<sub>3</sub>) δ 1.85-2.09 (m,2H), 2.32-2.56 (m,2H), 2.62 (broad d,2H), 5.64-5.79(m,1H), 6.23-6.38 (m,1H), 6.48-6.73 (m,2H). <sup>13</sup>C NMR (CCl<sub>4</sub>) δ 24.63, 30.28, 48.41, 128.41, 131.72, 132.24, 137.44. UV max (EtOH) 201 nm (ε 5040),

229 ( $\epsilon$  6660), 254 ( $\epsilon$  2190). Mass spectrum (EI)  $m/e$  (relative intensity) 118 (66.1%, M), 119 (5.36%, M+1), 117 (100%, M-1). Elemental analysis calc. for  $C_9H_{10}$ : C 91.47, H 8.53. Found: C 91.19, H 8.34.

2,3-Bis(ethoxycarbonyl)-2,3-diazabicyclo[2.2.1]hept-5-ene-7,5'-spirobicyclo[2.1.0]pentane (21). A sample of 20 (124 mg, 1.06 mmole) was dissolved in 3 ml dry benzene and 0.183 ml (1.16 mmole) of diethyl azodicarboxylate added. The mixture was refluxed under  $N_2$  for 12 hours and the solvent removed. The reaction mixture was dissolved in  $CH_2Cl_2$  and filtered through basic alumina. Removal of solvent gave 240 mg of 21 (78% yield).  $^1H$  NMR ( $CDCl_3$ )  $\delta$  1.30 (2t, 6H), 1.39-1.68 (m, 2H), 1.68-1.95 (m, 2H), 2.00-2.24 (m, 2H), 4.01-4.42 (m, 5H), 5.00-5.36 (broad s, 1H), 6.52-6.87 (broad s, 2H).  $^{13}C$  NMR ( $CDCl_3$ )  $\delta$  14.49, 19.43, 20.60, 24.50, 56.54, 62.45, 63.49, 67.33, 159.09. Mass spectrum (EI)  $m/e$  (relative intensity) 292 (0.750%, M), 293 (0.125%, M+1), 294 (0.0625%, M+2), 116 (100%, M-176).

2,3-Bis(ethoxycarbonyl)-2,3-diazabicyclo[2.2.1]heptane-7,5'-spirobicyclo[2.1.0]pentane (42a). A sample of 21 (295 mg, 1.01 mmole) was dissolved in 5 ml absolute ethanol and 0.400 ml (8.15 mmole) of hydrazine hydrate added. The mixture was heated to 55°C and left open to the atmosphere with stirring for 18 hours. Ethanol was removed by rotary evaporation and the product taken up in ether. The solution was extracted with distilled water until the aqueous layer was neutral by pH paper. The organic layer was then fil-



tered through basic alumina and the solvent removed to give 221 mg (74% yield) of 42a.  $^1\text{H}$  NMR ( $\text{CDCl}_3$ )  $\delta$  1.29 (t, 6H), 1.40-1.63 (m, 2H), 1.91 (broad s, 6H), 2.07-2.30 (m, 2H), 3.64 (broad s, 1H), 4.16 (q, 4H), 4.54 (broad s, 1H).  $^{13}\text{C}$  NMR ( $\text{CDCl}_3$ )  $\delta$  14.42, 20.27, 20.79, 21.11, 45.55, 58.28, 61.99, 62.90. Mass spectrum (EI) m/e (relative intensity) 294 (14.0%, M), 295 (2.38%, M+1), 296 (5.00%, M+2), 117 (100%, M-177).

2,3-Diazabicyclo[2.2.1]hept-2-ene-7,5'-spiro-bicyclo[2.1.0]pentane (19a). A solution of 1.40 g (25.0 mmole) potassium hydroxide in 10 ml isopropanol was brought to reflux under argon. Degassed isopropanol (12 ml) containing carbamate 42a (661 mg, 2.24 mmole) was added dropwise. Reflux was maintained for 2 hours. The solution was concentrated down to a light yellow paste which was taken up in 50 ml saturated sodium bicarbonate solution and extracted 5 times with methylene chloride. The organic layers were dried over sodium sulfate and left overnight in the dark in the presence of oxygen, after which solvent was removed. The crude diazene was sublimed at  $85^\circ$  and 0.1 torr then recrystallized from pentane. Yield 162 mg (49%).  $^1\text{H}$  NMR ( $\text{C}_6\text{D}_6$ )  $\delta$  0.58-1.33 (m, 8H), 1.50-1.69 (m, 2H), 3.84 (s, 1H), 4.75 (s, 1H).  $^{13}\text{C}$  NMR ( $\text{C}_6\text{D}_6$ )  $\delta$  19.91, 20.43, 21.21, 21.40, 21.53, 22.44, 48.24, 74.37, 78.79. UV max (EtOH) 207 nm ( $\epsilon$  501), 331 ( $\epsilon$  80.1), 338 ( $\epsilon$  79.1). Elemental

analysis calc. for  $C_9H_{12}N_2$ : C 72.94, H 8.16. Found: C 73.00, H 8.18.

Decomposition Studies of 19a. Compound 19a (ca. 12 mg, 0.08 mmole) was dissolved in 0.5 ml benzene- $d_6$  and placed in an NMR tube. The solution was degassed by 5 freeze-pump-thaw cycles and the tube sealed under vacuum. NMR spectra were taken at 15 minute intervals during the reactions. Analysis of the products was performed by gas chromatography on Column D (oven temperature 60-120°C, flow rate 50  $cm^3$   $N_2$ /min). GC/MS analysis confirmed that all products were  $C_9H_{12}$  isomers. Thermolysis: Tube was heated to 140°C in an oil bath for 3 hours. Direct photolysis: Tube was irradiated for 3 hours through a Pyrex filter. Sensitized photolysis: Sample was made up as above but also containing 41.8 mg benzophenone. The solution was photolyzed for 5.5 hours through a Corning LP-30 filter (cutoff 365 nm).<sup>38</sup>

Spiro[bis(bicyclo[2.1.0]pentane)-5,5'] (9). Product mixtures from direct photolysis of 19a were separated by preparative gas chromatography on Column B (oven temperature 100°C, gas flow 75  $cm^3$  He/min) to obtain a pure sample of 9.  $^1H$  NMR ( $C_6D_6$ )  $\delta$  1.45-1.73 (m, 4H), 1.94 (broad s, 4H), 2.00-2.22 (m, 4H).  $^{13}C$  NMR ( $C_6D_6$ )  $\delta$  18.22, 22.22, 22.31, 23.52, 35.59. Mass spectrum (EI) m/e (relative intensity) 120 (8.1%, M), 121 (1.2%, M+1), 91 (43.4%, M-29).

2,3-Divinylcyclopentene (24). 2,3-Divinylcyclopentene (24) was isolated from sensitized photolysate of 19 by preparative gas chromatography on Column B (oven temperature

110°, gas flow 75 cm<sup>3</sup> He/min). Spectral properties were identical to those reported in the literature.<sup>39</sup>

Reduction of 21 with Diimide-d<sub>2</sub>. A solution of carbamate 21 (140 mg, 0.478 mmole) and hydrazine hydrate-d<sub>6</sub> (0.250 ml, 5.09 mmole) in EtOD was stirred at 60° in the presence of oxygen for 16 hours. The solvent was removed and the residue taken up in ether. The organic layer was extracted with distilled water until the aqueous layer was neutral to pH paper. Filtration through basic alumina and removal of the solvent gave 139 mg of 42b (98% yield). <sup>2</sup>H NMR (C<sub>6</sub>H<sub>6</sub>) δ 1.41 (broad s).

Synthesis of 19b. Carbamate-d<sub>2</sub> (42b, 501 mg, 1.69 mmole) was subjected to the hydrolysis-oxidation procedure described above to yield 123 mg of 19b (48% yield). <sup>2</sup>H NMR (CCl<sub>4</sub>) δ 1.52 (s,exo).

Addition of PTAD to 19b. N-phenyltriazolinedione (250 mg, 1.43 mmole) was added to a solution of 19b (109 mg, 0.725 mmole) in 5 ml benzene. The reaction mixture was stirred under argon at 50° for 2 days, then water was added and the solution reheated until the red color of PTAD disappeared. The resulting yellow solution was extracted 3 times with saturated sodium bicarbonate solution then with distilled water until neutral to pH paper. After drying with sodium sulfate, the solvent was removed to give 226 mg of adduct 31 (96% yield). <sup>1</sup>H NMR (CDCl<sub>3</sub>) δ 1.08 (s,2H),

1.49 (s,1H), 1.87 (s,3H), 3.89 (s,1H), 4.07 (s,1H), 4.73 (s,1H), 4.96 (s,1H), 7.39 (s,5H).

Solid State Photolysis of 31. Adduct 31 (226 mg, 0.692 mmole) was divided into 10-5 mm o.d. Pyrex tubes and photolyzed under argon for 6 days.  $^1\text{H}$  NMR confirmed that the reaction had reached >95% completion. Yield of 43 was 198 mg (96%).  $^2\text{H}$  NMR ( $\text{C}_6\text{H}_6$ )  $\delta$  0.88 (endo), 1.43 (endo), 1.62 (exo), 1.77 (exo). Solution phase thermolysis and photolysis both lead to complete  $^2\text{H}$  scrambling.

Synthesis of 19c. A solution of 0.37 g (6.6 mmole) potassium hydroxide in 6 ml isopropanol was brought to reflux under argon and a suspension of 198 mg (0.665 mmole) urazole 43 in 40 ml degassed isopropanol was added dropwise. Reflux was maintained for 2.5 hours and the solvent removed to give a brown paste which was taken up in saturated sodium bicarbonate solution, extracted 5 times with methylene chloride, and dried with sodium sulfate. After exposure to air in the dark overnight, evaporation of solvent gave a yellow oil from which 19c was purified by preparative gas chromatography on Column A (oven temperature  $90^\circ$ , gas flow  $100\text{ cm}^3\text{ He/min}$ ). Yield of 19c was 44.2 mg (44%).  $^2\text{H}$  NMR ( $\text{CCl}_4$ )  $\delta$  1.24 (0.80D, endo), 1.39 (0.80D, endo), 1.95 (0.20D, exo), 1.98 (0.20D, exo).

2,3-Divinylcyclopentene- $\text{d}_2$ . 2,3-Divinylcyclopentene- $\text{d}_2$  was isolated from the sensitized photolysate of 19b or 19c as described above for unlabeled material.  $^2\text{H}$  NMR ( $\text{CCl}_4$ )  $\delta$  1.56 (D4, trans), 1.98 (D4, cis), 2.13 (D5, cis), 2.25 (D5, trans), 4.78 (vinyl), 4.85 + sh (vinyl), 4.99 (vinyl).

Deuterium is labeled as cis or trans with respect to the proton on C3 (See Figures 3 and 4). Relaxation ( $T_1$ ) studies ensured that the integrals were reliable. Signal assignments for 24 were based on extensive decoupling and NOE experiments using 500-MHz  $^1\text{H}$  NMR.

Control Experiment for the Stability of Hydrocarbon Products to Sensitized Photolysis. A solution of 19a (2.49 mg, 0.0168 mmol) and 0.1  $\mu\text{l}$  undecane as an internal standard in 0.4 ml benzene was degassed by bubbling argon through for 10 minutes.<sup>40</sup> The solution was photolyzed and aliquots were removed every 30 min. for analysis by gas chromatography on Column B (oven temperature 60–120°, gas flow 50  $\text{cm}^3 \text{N}_2/\text{min}$ ). When the reaction reached 50% completion (1.5 hr), a solution of 11.0 mg (0.0604 mmol) benzophenone in 0.2 ml benzene was added and the solution degassed again. Photolysis was then performed through a Corning LP-30 filter. Analysis continued as described above. After 3.5 hr total photolysis the concentration of triene 24 and the unidentified  $\text{C}_9\text{H}_{12}$  product declined with further photolysis while the concentration of 9 remained constant.

Control Experiment for Rearrangement of 19c During Sensitized Photolysis. Diazene 19c (8.00 mg, 0.053 mmol) was dissolved in 0.5 ml benzene- $\text{d}_6$  and 10.8 mg (0.059 mmol) benzophenone was added. The solution was placed in an NMR tube, degassed by 3 freeze-pump-thaw cycles and sealed under

vacuum. The mixture was photolyzed through a Corning LP-30 filter until NMR analysis showed 41% decomposition of 19c. The remaining diazene was isolated by preparative gas chromatography on Column A (oven temperature 85°, gas flow 100 cm<sup>3</sup> He/min). <sup>2</sup>H NMR revealed no 19b. The endo:exo ratio in the recovered 19c was 3.94:1 (starting material 3.97:1).

Addition of PTAD to 20. Diene 20 (471 mg, 3.98 mmole) was dissolved in benzene and 2.09 g (11.9 mmole) N-phenyl-triazolinedione added. The solution was heated to 60° and reaction followed by TLC until complete after 6 days. The solvent was removed and the products chromatographed on silica gel (EM Silica Gel 60, 70-230 mesh), eluting with 10% EtOAc/CHCl<sub>3</sub>, to give 590 mg of bisurazole 22 (32% yield). <sup>1</sup>H NMR (CDCl<sub>3</sub>) δ 1.81-2.07 (m, 4H), 4.08 (s, 1H), 4.62 (s, 1H), 4.82 (s, 1H), 5.13 (s, 1H), 6.57 (qt, 2H), 7.39 (s, 5H), 7.45 (s, 5H). <sup>13</sup>C NMR (CDCl<sub>3</sub>) δ 25.40, 26.51, 60.62, 64.91, 78.43, 78.95, 125.35, 125.36, 125.48, 128.54, 129.25, 130.29, 130.94, 131.33, 132.63, 155.18, 155.31, 157.91, 158.30.

Reduction of 22. A solution of 360 mg (0.769 mmole) bisurazole 22 in 200 ml ethyl acetate was hydrogenated at atmospheric pressure using palladium on carbon as catalyst. Yield was 290 mg of 44 (80%). <sup>1</sup>H NMR (CDCl<sub>3</sub>) δ 2.08 (broad s, 8H), 4.32 (s, 2H), 4.55 (s, 2H), 7.48 (broad s, 10H). <sup>13</sup>C NMR (CDCl<sub>3</sub>) δ 26.77, 26.90, 59.98, 60.31, 71.62, 125.36, 128.61, 129.33, 131.38, 155.32, 155.78.

Spiro[bis(2,3-diazabicyclo[2.2.1]hept-2-ene)-7,7']

(17). A solution of 0.49 g (8.73 mmole) potassium hydroxide in 30 ml degassed isopropanol was brought to reflux under argon and a suspension of 197 mg (0.419 mmole) bisurazole 44 in 125 ml isopropanol added dropwise. Reflux was maintained for 3 hours and the solvent removed to yield a yellow paste which was taken up in 95% ethanol. Saturated copper(II) chloride solution was added until a dark brown precipitate formed. The precipitate was collected and dissolved in 50 ml of 25% ammonium hydroxide, which was extracted 6 times with methylene chloride. Drying over sodium sulfate and removal of solvent gave a yellowish solid from which the bisdiazene 17 was sublimed at 0.5 torr and 100°. Yield was 65.5 mg (89%). The compound was further purified by recrystallization from methylene chloride/hexane.  $^1\text{H}$  NMR ( $\text{C}_6\text{D}_6$ )  $\delta$  0.32-1.11 (m, 8H), 3.93 (m, 2H), 4.17 (m, 2H).  $^{13}\text{C}$  NMR ( $\text{CD}_2\text{Cl}_2$ )  $\delta$  19.42, 20.33, 74.14, 76.09, 76.94. UV max (EtOH) 224 nm ( $\epsilon$  520), 334 ( $\epsilon$  84), 342 ( $\epsilon$  86). Elemental analysis calc. for  $\text{C}_9\text{H}_{12}\text{N}_4$ : C 61.34, H 6.86, N 31.79. Found: C 61.09, H 6.89, N 31.80.

Direct Photolysis of 17. A solution of 17 (1.00 mg, 0.00567 mmole) in 0.5 ml benzene- $\text{d}_6$  was degassed by bubbling argon through for 15 minutes and capped with a septum.<sup>43</sup> The sample was irradiated through a Pyrex filter. Aliquots were removed at 15 minute intervals and analyzed by gas

chromatography on Column D (oven temperature 50-120°, gas flow 75 cm<sup>3</sup> N<sub>2</sub>/min).

Sensitized Photolysis of 17. Compound 17 (0.75 mg, 0.00426 mmole) was dissolved in 0.075 ml of 0.250 M benzophenone in benzene. 0.3 μl n-Undecane was added as an internal standard. The solution was placed in a 3 mm o.d. Pyrex tube, degassed by bubbling argon through for 15 minutes, and capped with a septum. The sample was irradiated through a Corning 0-52 filter<sup>38</sup> and aliquots taken every 30 minutes for analysis by gas chromatography on Column D (oven temperature 50-150°, gas flow 75 cm<sup>3</sup> N<sub>2</sub>/min).

8,9-Diazatricyclo[5.2.2.0<sup>2,6</sup>]undeca-2,8-diene (23).

Diazene 17 (14.0 mg, 0.0795 mmole) was dissolved in 1.00 ml 0.250 M benzophenone in benzene and placed in an 8 mm o.d. Pyrex tube. The sample was degassed by 4 freeze-pump-thaw cycles and irradiated for 2.5 hours through a Corning 0-52 filter.<sup>38</sup> The products were isolated by preparative gas chromatography on Column C (oven temperature 120°, gas flow 100 cm<sup>3</sup> He/min). The isolated yield of 23 was 0.60 mg (5.1%). <sup>1</sup>H NMR (C<sub>6</sub>D<sub>6</sub>) δ 0.65-2.20 (m, 9H), 4.94 (broad s, 1H), 5.15 (broad s, 1H), 5.49 (broad s, 1H). <sup>13</sup>C NMR (C<sub>6</sub>D<sub>6</sub>) δ 13.94, 28.46, 29.27, 34.12, 45.41, 65.36, 68.05, 120.79, 143.83. UV max (EtOH) 227 nm (ε 1230), 375 (ε 51). Mass spectrum (EI) m/e (relative intensity) 120 (27.7%, M-N<sub>2</sub>), 121 (2.3%, M+1-N<sub>2</sub>).



Sensitized Photolysis of 23. Compound 23 (0.17 mg, 0.00115 mmole) was dissolved in 0.125 ml 0.250 M benzophenone in benzene, degassed by bubbling argon through for 10 minutes and capped with a septum. The sample was photolyzed for 20 minutes through a Corning 0-52 filter<sup>38</sup> and analyzed by gas chromatography on Column E (oven temperature 50-150°, H<sub>2</sub> carrier gas, linear velocity 40 cm/sec.)

Quantum Yields. The azo compound (0.075 mmole) was dissolved in 1.00 ml 0.25 M benzophenone in benzene and placed in one of a set of three labeled 8 mm o.d. Pyrex tubes. One sample in each run consisted of 2,3-diazabicycloheptene<sup>5,12</sup> (5) as an actinometer. Solutions were degassed by 5 freeze-pump-thaw cycles and placed in a merry-go-round where they were irradiated to ca. 10% conversion through a Corning 0-52 filter. Control experiments confirmed that the sample tubes had identical optical properties and that no direct photolysis occurred under the experimental conditions. Nitrogen produced upon irradiation was measured by pumping the gas into a calibrated gas buret using a Toepler pump. Disappearance of the azo compound was measured by gas chromatography on Column E or F (oven temperature 50-150°, H<sub>2</sub> carrier gas, linear velocity 40 cm/sec) using the benzophenone sensitizer as an internal standard. If both nitrogen measurement and GC analysis were required, separate runs were performed for each.

The exception to the above procedure was compound 14, for which 0.94 mg (0.00634 mmole) 14 and 0.98 mg

(0.00661 mmole) 8a were dissolved together in 0.250 ml of 0.250 M benzophenone in benzene and the solution degassed by 5 freeze-pump-thaw cycles. Irradiation was performed as described above and analysis done by gas chromatography on Column F (conditions above) using 8a as an internal actinometer and the benzophenone as an internal standard.

2,3-Diazabicyclo[2.2.1]hept-2-ene-7-spirocyclopropane (26). Compound 26 was synthesized by the method of Roth.<sup>14</sup>

Preparation of ESR Samples. Samples were prepared by adding sufficient quantities of the diazene to 0.3-0.5 ml purified 2-methyltetrahydrofuran to reach the concentrations listed in Table XIII. For experiments involving sensitized photolysis, benzophenone was then added to reach the desired concentration. The solutions were placed in 5 mm o.d. quartz ESR tubes equipped with high vacuum stopcocks. The tubes were then degassed by 5 freeze-pump-thaw cycles and frozen in liquid nitrogen before being inserted into the precooled ESR cavity.

ESR Experiments. A Varian E-9 spectrometer was outfitted with both an Air Products and Chemicals Helitran liquid helium transfer apparatus and an Oriel 200-W mercury-xenon lamp, which was focused into the microwave cavity. The output of the lamp, which was generally operated at 120-150 W, was filtered through water and Pyrex.

Before each experiment, the temperature at the sample was checked with a calibrated thermocouple sealed in a

sample tube. The temperature was then monitored throughout the experiment with a less accurate thermocouple fixed 1 cm below the sample in the quartz Dewar. Heating above the minimum temperature (about 8°K) was achieved by adjusting either the helium flow rate or the Helitran automatic temperature controller.

REFERENCES AND NOTES FOR CHAPTER III.

1. (a) Michl, J., Ed., Tetrahedron, 1982, 38, 733-868.  
(b) Borden, W. T., Ed., "Diradicals", Wiley, New York, 1982.
2. Engel, P. S., Chem. Rev., 1980, 80, 99-150; Adam, W. and DeLucchi, O., Angew. Chem. Int. Ed. Engl., 1980, 19, 762-779.
3. Buchwalter, S. L. and Closs, G. L., J. Am. Chem. Soc., 1979, 101, 4688-4694.
4. Semmelhack, M. F.; Foos, J. S.; Katz, S., J. Am. Chem. Soc., 1973, 95, 7325-7336.
5. Gassman, P. G., Mansfield, K. T. in "Organic Syntheses", Vol. 49, Wiberg, K. B., Ed., Wiley, NY, 1969, pp. 1-6.
6. Semmelhack, M. F.; Weller, H. N.; Foos, J. S., J. Am. Chem. Soc., 1977, 99, 292-294.
7. Rylander, P., "Catalytic Hydrogenation in Organic Syntheses", Academic Press, New York, 1979, pp. 251-254.
8. Greenberg, A. and Liebman, J. F., "Strained Organic Molecules", Academic Press, New York, 1978, 178-202.
9. Roth, W. R.; Martin, M., Tet. Lett., 1967, 4695-4698; Chang, M. H.; Dougherty, D. A., J. Org. Chem., 1981, 46, 4092-4093.
10. We have also developed another synthetic route to 17 which is longer but more amenable to large scale.  
Anderson, J. A., Masters Thesis, California Institute of Technology, 1983.

11. Doubleday, C., Jr.; McIver, J. W., Jr; Page, M.,  
J. Am. Chem. Soc., 1982, 104, 6533-6542.
12. Engel, P. S., J. Am. Chem. Soc., 1969, 91, 6903-6907.
13. Clark, W. D. K.; Steel, C., Jr., J. Am. Chem. Soc.,  
1971, 93, 6347-6355.
14. Roth, W. R.; Enderer, K., Justus Liebigs Ann. Chem.,  
1970, 733, 44-58.
15. Gajewski, J. J., "Hydrocarbon Thermal Isomerizations",  
Academic Press, New York, 1980, (a) pp. 94-104,  
(b) pp. 315-333.
16. Steel, C.; Zand, R.; Hurwitz, P.; Cohen, S. G.,  
J. Am. Chem. Soc., 1964, 86, 679-684.
17. Doering, W. von E.; Gilbert, J. C., Tetrahedron, Suppl.,  
1966, 7, 397-414.
18. Roth, W. R.; Enderer, K., Justus Liebigs Ann. Chem.,  
1969, 730, 82-90. Roth, W. R.; Martin, M.,  
Justus Liebigs Ann. Chem., 1967, 702, 1-7.
19. Beckwith, A. L. J.; Ingold, K. U. in "Rearrangements  
in Ground and Excited States", de Mayo, P. D., Ed.,  
Academic Press, NY, 1980, Vol. 1, (a) p. 180,  
(b) pp. 227-235.
20. Chapman, O. L., personal communication.
21. Connell, A. C.; Whitham, G. H., J. Chem. Soc., Perkin I,  
1983, 989-994.
22. Suzuki, M.; Murahashi, S.-I.; Sonoda, A.; Moritani, I.,  
Chem. Lett., 1974, 267-270.

23. Porter, N. A.; Nixon, J. R., J. Am. Chem. Soc., 1978, 100, 7116-7117. Porter, N. A.; Cudd, M. A.; Miller, R. W.; McPhail, A. T., Ibid, 1980, 102, 414-416.
24. McIver, J. W., Jr., Accts. Chem. Res., 1974, 7, 72-77.
25. Wertz, J. E.; Bolton, J. R., "Electron Spin Resonance: Elementary Theory and Practical Applications", McGraw-Hill, New York, 1972.
26. Goldberg, A. H., Masters Thesis, California Institute of Technology, 1982.
27. Lokensgard, D. M.; Berson, J. A., unpublished results.
28. Jain, R.; Dougherty, D. A., unpublished results.
29. Masek, B. B., unpublished results.
30. Senthilnathan, V. P.; Platz, M. S., J. Am. Chem. Soc., 1980, 102, 7637-7643.
31. Berson, J. A. in reference 1b, pp. 151-194 and references therein.
32. Engel, P. S.; Keys, D. E., J. Am. Chem. Soc., 1982, 104, 6860-6861.
33. Cope, A. C.; Stevens, C. L.; Hochstein, F. A., J. Am. Chem. Soc., 1950, 72, 2510-2514. Cope, A. C.; Haven, A. C., Jr.,; Ramp, F. L.; Trumbull, E. R., J. Am. Chem. Soc., 1952, 74, 4867-4871.
34. Weil, T.; Cais, M., J. Org. Chem., 1963, 28, 2472.
35. An explosion during the distillation of diazocyclopentadiene has been reported<sup>36</sup> but this occurred

at 47°C and 48 torr. We have encountered no difficulties during trap-to-trap distillations as described.

36. Ramirez, F.; Levy, S., J. Org. Chem., 1958, 23, 2036-2037.
37. Still, W. C.; Kahn, M.; Mitra, A., J. Org. Chem., 1978, 43, 2923-2925.
38. Control experiments confirmed that direct photolysis did not occur through the filters used in sensitization experiments.
39. Connell, A. C.; Whitham, G. H., J. Chem. Soc., Perkin I., 1983, 989-994. Untch, K. G.; Martin, D. J., J. Am. Chem. Soc., 1965, 87, 4501-4506. Skattebol, L.; Solomon, S., J. Am. Chem. Soc., 1965, 87, 4506-4513.
40. There has been a recent criticism of deoxygenation by bubbling inert gas through solvents.<sup>41</sup> In our hands samples degassed by several freeze-pump-thaw cycles and those deoxygenated with argon have given identical results. However, it is indicated in this section which method was used for each experiment.
41. Skell, P. S.; Tlumak, R. L.; Seshadri, S., J. Am. Chem. Soc., 1983, 105, 5125-5131.